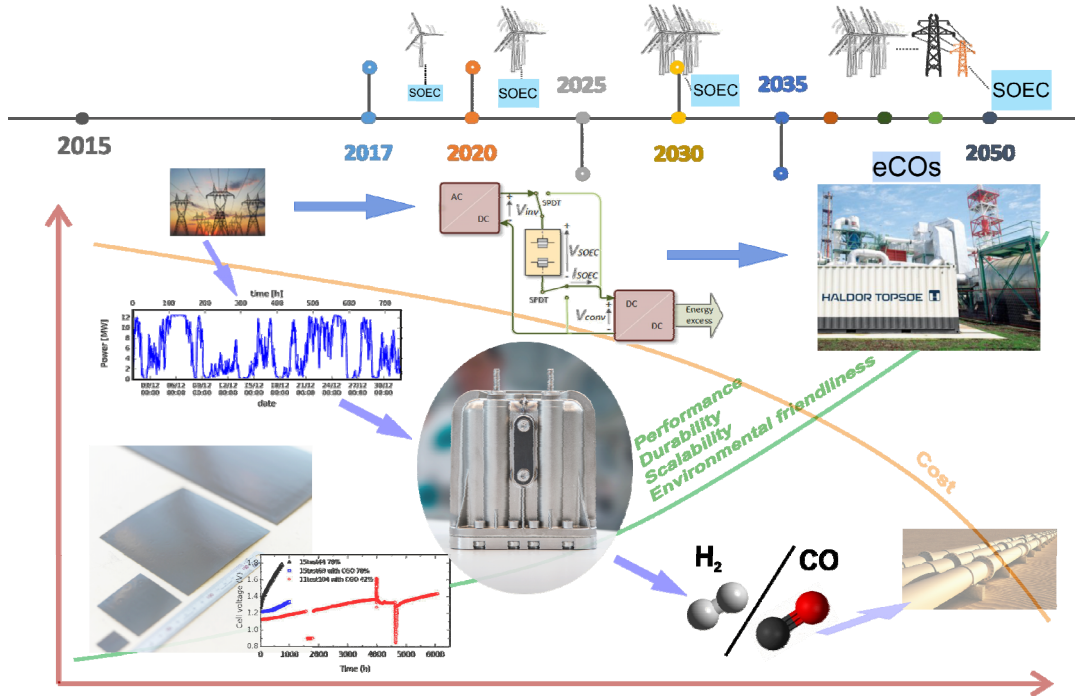


Final report for

ForskEL 2015-1-12276 Towards Solid Oxide Electrolysis Plants in 2020



Report compiled by: Ming Chen

Contributors:

Department of Energy Conversion and Storage, Technical University of Denmark (DTU Energy):

Ming Chen, Anne Hauch, Xiufu Sun, Karen Brodersen, Peter Stanley Jørgensen, Janet Jonna Bentzen, Simona Ovtar, Xiaofeng Tong, Theis Løye Skafte, Christopher R. Graves, Sebastian Molin, Kawai Kwok, Li Han, Jens Valdemar Thorvald Høgh, Philipp Zielke, Karsten Agersted, Jón Steinar Garðarsson Mýrdal

Haldor Topsøe A/S (HTAS):

Peter Blennow, Rainer Küngas

Department of Development and Planning, Aalborg University (AAU):

Brian Vad Mathiesen, Iva Ridjan, Andrei David

Department of Electrical Engineering, Technical University of Denmark (DTU Elektro):

Zhe Zhang, Alexander Anthon, Yudi Xiao, Pierre Pinson, Yunpeng Xiao

1.1 Project details

Project title	Towards Solid Oxide Electrolysis Plants in 2020
Project identification (program abbrev. and file)	Energinet.dk project no. 2015-1-12276
Name of the programme which has funded the project	ForskEL
Project managing company/institution (name and address)	Department of Energy Conversion and Storage, Technical University of Denmark (DTU Energy) DTU Risø Campus, Frederiksborgvej 399, 4000 Roskilde, Denmark
Project partners	Haldor Topsøe A/S (HTAS) Department of Development and Planning, Aalborg University (AAU) Department of Electrical Engineering, Technical University of Denmark (DTU Elektro)
CVR (central business register)	DK30060946
Date for submission	2017-09-08

1.2 Short description of project objective and results

1.2.1 *Danish version*

1.2.2 *English version*

1.3 Executive summary

1.4 Project objectives

1.5 Project results and dissemination of results

1.5.1 *Overview and milestones*

1.5.2 *WP1 – Cell development and testing*

1.5.3 *WP2 – Stack components and interfaces*

1.5.4 *WP3 – Stack development and testing*

1.5.5 *WP4 – SOEC system*

1.5.6 *WP5 – Energy system modelling*

1.5.7 *Dissemination of project results*

1.5.8 *Environmental benefits of the project*

1.6 Utilization of project results

1.7 Project conclusion and perspective

1.2 Short description of project objective and results

1.2.1 Danish version

Dette projekts formål var at forbedre SOEC-teknologien yderligere, med det ultimative mål at gøre teknologien klar til at være en vigtig aktør i overgangen til vedvarende energi. Vi har vist stabil drift ved elektrolysebetingelser i mere end et år og demonstreret hvordan store SOEC stakke kan anvendes problemfrit til netbalanceringsformål. I projektet har vi forbedret SOEC fra stabil drift op til -1 til nu -1.25 A/cm² og forbedret stak- og systemdesign er blevet valideret og implementeret i produktion. Desuden har vi udviklet en billigere og mere effektiv strømkonverter samt etableret en dansk køreplan for storskalaimplementering af elektrolyse-systemer. Disse resultater er i tråd med den danske strategi for SOEC og har bidraget væsentlig til kommercialiseringen af dansk SOEC-teknologi.

1.2.2 English version

This project aimed to further improve the SOEC technology, with an ultimate goal of making it ready as a key player in the transition to renewable energy. We have demonstrated stable electrolysis operation for more than one year and have shown large SOEC stacks can be operated smoothly for grid balancing purposes. We pushed stable operating point for SOEC cells from -1 to -1.25 A/cm². Improved stack and system designs were validated and implemented into production. Besides, we have developed a power converter with improved efficiency and lower cost and have established a Danish roadmap for large scale implementation of electrolyzers. These results are in line with the Danish national strategy on SOEC and have contributed significantly to the commercialization of the Danish SOEC technology.

1.3 Executive summary

The future Danish power (electricity) system will be based on a high amount of fluctuating renewable energy (RE) and will therefore require inexpensive, efficient power storage and/or regulation technologies. High temperature electrolysis based on solid oxide electrolysis cells is a very promising technology for energy storage and production of synthetic fuels. It has a unique possibility for grid regulation in the future Danish power system. The goal of this 2-year project was to further improve performance and durability of SOEC cells and stacks targeting applications specifically for regulating the future Danish power system, and at the same time enhance the cost competitiveness and environmental friendliness of the SOEC technology, with an ultimate goal of making the SOEC technology ready as a key player in the transition to renewable energy available from around 2020. The four project partners (DTU Energy, Haldor Topsøe A/S, DTU Elektro, and Aalborg University) have been working closely on the following critical research issues: further improvement of SOEC cell performance and durability at a current density above -1.25 A/cm^2 and its carbon tolerance, development of robust and reliable stack component interfaces enabling stable stack operation for grid balancing applications, technical analysis of the implications of the Danish power grid and implications of power electronics on SOEC stacks, establishment of schematic designs of future SOEC plants, and from an energy system perspective creation of a Danish roadmap for the development and implementation of large-scale electrolyzers. Progress on all these critical issues is necessary for SOECs to become a key player of the future Danish energy system.

In the previous project ForskEL 2013-1-12013 "Solid Oxide Electrolysis for Grid Balancing", we developed cells (2014 generation) which were capable of electrolysis operation up to -1 A/cm^2 , demonstrating a long-term degradation rate of 0.3-0.4 %/1000 h in a 2000 h cell test. At the stack level, we demonstrated that reversible SOEC stacks can be operated in a stable manner with a real-world relevant operating profile for grid balancing purpose. In addition, a new stack design (TSP-1, 2014 generation) was developed and tested, being superior to the old design (Delta) on several aspects. A number of long-term stack tests were conducted for periods up to 1800 h, showing stable electrolysis performance and good durability of the new stack design. The above represents the starting point for the cell and stack development work in this project.

In WP1 of this project we first evaluated lifetime performance of 2014 generation SOEC cells and stacks using a grid balancing scheme simulating 100 % absorption of wind power. Both single cell and stack test results indicated that the wind profile run caused no additional degradation. The cell and stack durability was further studied under long-term steady state electrolysis operation. The longest SOEC single cell test completed in this project has reached 9000 h, whereas the longest record for single stack test is 10,400 h. It can be concluded that the lifetime of 2014 generation SOEC cells is beyond one year (at $800 \text{ }^\circ\text{C}$ and -1 A/cm^2) and there are indications on lifetime exceeding 2 years (at equivalent or less harsh conditions). Extensive efforts were further devoted to improving cell durability at -1.25 A/cm^2 . Through detailed post-mortem analyses and advanced 3D electrode structure characterization on tested cells, we identified the Ni/YSZ electrode as the main cause of the degradation and confirmed its microstructure change in correlation with the hydrogen/steam flow direction. To counter-act the degradation, we introduced different electro-catalysts into the Ni/YSZ electrode. We were able to bring down the cell degradation by a factor of 15, from 714 mV (60 %) to 50 mV (4 %) per 1000 h. The single cell test has been running for more than 6000 h. Another achievement is on enhancing carbon tolerance, where we developed SOEC cells with a Ni-free fuel electrode, showing completely stable performance and no sign of carbon deposition when exposed to carbon deposition inducing condition. Besides, the environmental friendliness of the cell production process was also improved with the cell performance reaching the project target.

WP2 focused on stack components and their interfaces. We looked into the corrosion of interconnects (ICs) in reducing atmospheres resembling the fuel side environment of SOEC stacks. For electrolysis of steam, this side of ICs is exposed to high steam content, e.g.

$H_2O/H_2 = 90/10$, and its corrosion behaviour is of concern. By applying a Y (yttrium) coating developed in this project, a corrosion rate of $0.2 \times 10^{-14} \text{ g}^2 \text{ cm}^{-4} \text{ s}^{-1}$ was achieved when the coated ICs were exposed to 90 % H_2O in H_2 at 750 °C. For the oxygen side, the MnCo spinel ($(Co,Mn)_3O_4$) coating by electrophoretic deposition developed in the previous project was improved. Further enhancement of the corrosion resistance was achieved by applying a second layer Y coating (between the steel IC and the EPD spinel coating) using electrolytic deposition (ELD). The Y+MCO dual-layer coated ICs demonstrated a corrosion rate constant of $0.52 \times 10^{-14} \text{ g}^2 \text{ cm}^{-4} \text{ s}^{-1}$ from a 4000 h corrosion test at the component level and of $0.72 \times 10^{-14} \text{ g}^2 \text{ cm}^{-4} \text{ s}^{-1}$ from a 7000 h corrosion test on full size ICs ($12 \times 12 \text{ cm}^2$), both at 800 °C in air. The other part of WP2 dealt with stack component interfaces in SOEC stacks. The oxygen electrode-IC interface was considered as one of the weakest interfaces in the 2014 generation SOEC stacks. The peeling stress at this interface was calculated and the occurrence of contact loss was estimated. Limits of operating conditions with regard to free of contact loss were proposed. By replacing the standard contact component at the oxygen electrode – IC joint with a CuMn foam, we increased the interface fracture energy by a factor of >2 .

In WP3, extensive stack development and testing was carried out, focusing on HTAS' TSP-1 stack design. Performance and durability of the 2014 generation stacks was evaluated under different conditions, including different transient modes with both load and temperature cycles, different temperatures and current densities, and for electrolysis of steam or CO_2 , or co-electrolysis of steam and CO_2 , with the longest test period exceeding 10,000 h. One of the stack tests was to simulate 100 % wind power absorbing, where the TSP-1 stack followed a real-world wind power production profile quite well showing no additional degradation caused by dynamic operation. It was concluded that the TSP-1 stacks (as per 2014 generation) will have a lifetime of at least one year and there are indications on lifetime exceeding two years. A total degradation rate of 20 mV or approximately 1.4 % per 1000 h was demonstrated in the 10,400 h stack test completed in the current project. Further improvement at the stack level was achieved via improving gas flow distribution and applying a new contact layer for the oxygen electrode side. The new stack design, called TSP-1.3, has been validated and implemented in SOEC stack production at HTAS.

The focus of WP4 shifts to SOEC systems. We first looked into electrolyser participation in electricity markets with both transmission- and distribution-level applications, analyzed optimal size, voltage level, and participating strategy of electrolysers, based on these proposed scenarios regarding deployment of electrolysers in the Danish electricity grid. We further proposed two schematic designs of future SOEC plants, one on SOEC steam electrolysis for hydrogen production and the other on reversible SOEC plant for full energy system balancing. In WP4, we also worked on the actual SOEC-CORE system. The casing temperature of SOEC stacks in a SOEC-CORE was measured at various operating points and compared with the COMSOL stack model. Based on the obtained results, an improved SOEC-CORE system (with respect to improved heat distribution, lower pressure drops across components etc.) was developed and validated in this project. The test results confirmed improved thermal insulation of the new CORE design. For SOEC/SOFC reversible operation, a costly bi-directional AC-DC power supply unit (PSU) is required. The PSU consists of an AC-DC rectifier and a bi-directional DC-DC converter. We developed a novel power control unit (PCU) architecture and achieved a much more symmetrical power operating range for the DC-DC converter (as compared to conventional ones). The newly developed converter demonstrated a maximum efficiency of 96.5 %. Its control was further tested with a 14-cell SOEC stack, showing promising results and potential in integration into SOEC-CORE systems.

The last work package of this project (WP5) focused on energy system modelling. We first assessed the role of electrolysers on electricity markets for both short-term and long-term. We concluded that electrolysis should be primarily for electrofuel production, as it can provide the missing link between intermittent renewable energy, resource scarcity and dependence on high-density fuels. A Danish roadmap for large-scale implementation of electrolysers was established in this project. The roadmap was divided into four main stages, covering the period from now on to beyond 2035. It summarized different activities, measures and incentives that should be implemented in order to speed up and maximize the implementation of electrolysis. Finally we developed a technology data sheet for the production of synthetic

fuels. The involved technologies and their development status were reviewed, and their potential and overall investment costs were assessed.

As compared to the previous projects, significant progresses have been achieved in this project with respect to the SOEC technology development. With the 2014 generation technology, we have demonstrated stable electrolysis operation for more than one year, both at the cell level and at the stack level. We have also shown that the cells and stacks can be operated in a stable manner under grid balancing related conditions, with a realistic wind power production profile. By introducing electrocatalysts into the Ni/YSZ electrode, we were able to push the operating point for SOEC cells from -1 to -1.25 A/cm² with on-going cell tests running for more than 6000 h. At the stack level, we have further improved the gas flow distribution and the interface adherence and the new stack design is now implemented in HTAS stack production. The results obtained in this project are in line with the Danish national strategy and roadmap on SOEC and has further contributed to the commercialization of the SOEC technology at HTAS. Along with this series of ForskEL projects, HTAS has now matured its on-site carbon monoxide generation technology (based on electrolysis of CO₂) to a small-plant level¹. This achievement is an important stepstone in commercialization of the SOEC technology, towards the ultimate goal of making it ready as a key player in the transition to renewable energy available from around 2020.

1.4 Project objectives

The overall objective of this project was to further improve performance and durability of SOEC cells and stacks and at the same time enhance the cost competitiveness and environmental friendliness of the SOEC technology, with an ultimate goal of making the SOEC technology ready as a key player in the transition to renewable energy available from around 2020. To facilitate monitoring progress towards the overall project targets, 24 milestones were formulated in the original project plan, specifying explicitly the project targets with regard to the SOEC technology development. A list of these milestones and their status at the completion of the project can be found in Section 1.5.1 of this report. At the end of this project, we have fulfilled 18 out of the 24 milestones and have partially fulfilled the rest six milestones. Overall we have achieved the project targets to a great extent.

Along with the project course most of the tasks were carried out according to the project plan, though a number of technical challenges and deviations from the original plan were encountered still. One of the challenges lied in the work planned in WT2.2 and WT4.2. The milestone M2.4 in WT2.2 was formulated based on the old HTAS stack design (Delta), where the described interface "end-plate-braze-IC joint" was problematic. This problem was however resolved already after introducing the new HTAS stack design (TSP-1). During the time the project proposal was written, this progress was not foreseen. M2.4 became irrelevant after the project started. Instead of sticking to the original Milestone M2.4, we proposed to devote resources to improve the oxygen electrode-IC interface, which was considered (by all stakeholders) as one of the weakest interfaces. A new milestone M2.6 on improving the fracture toughness of this critical interface was proposed and the change to the project plan was approved. At the end of this project, by using a CuMn foam as the contact component, we have successfully increased the interface fracture energy by a factor of >2. The introduction of the new TSP-1 stack design also influenced the work in WT4.2. There it was originally planned to work on optimizing the design of electrical heaters. These activities no longer reflected the actual need at HTAS for further stack technology development based on the new TSP-1 design. Modifications to WT4.2 were hence proposed and efforts were devoted to improving the SOEC-CORE system design, which was one of the critical topics towards the overall project target, i.e. "Towards SOEC plants in 2020".

¹ <http://blog.topsoe.com/2016/12/site-carbon-monoxide-generation-takes-next-step>

1.5 Project results and dissemination of results

1.5.1 Overview and milestones

The project was structured into five technical work packages (WPs), which were further divided into a number of work tasks (WTs) as listed below:

WP1 – Cell development and testing

- WT1.1 – Grid balancing related single cell testing
- WT1.2 – Advanced 3D structure characterization
- WT1.3 – Optimized SOEC cells with enhanced durability
- WT1.4 – Optimized SOEC cells with enhanced carbon tolerance

WP2 – Stack component and interfaces

- WT2.1 – Durable and cheap interconnects (ICs)
- WT2.2 – Robust and reliable stack component interfaces

WP3 – Stack development and testing

- WT3.1 – Grid balancing related stack testing
- WT3.2 – SOEC stack testing of improved cell and stack components

WP4 – SOEC system

- WT4.1 – Schematic designs of future SOEC plants
- WT4.2 – Key system components

WP5 – Energy system modelling

Further listed below are the milestones that were set up in the project plan and their status at the completion of the project:

M1.1 Life-time of the 2014 generation SOEC cells under the representative SOEC operation schemes identified in WT4.1 (which fulfils the technical requirements for the Danish power grid for grid balancing) predicted.

[Milestone fulfilled. We investigated performance and durability of the 2014 generation SOEC cells via both single cell testing and stack testing, under steady state electrolysis operation and dynamic operation simulating 100 % absorbing of wind power. The results show that the cell lifetime is beyond one year and that there are indications on lifetime exceeding two years. The dynamic operation scheme employed in the current project seems having not introduced any additional degradation.]

M1.2 3D reconstruction and microstructure analysis of long-term tested SOEC electrodes and corresponding reference carried out and quantitative 3D descriptions reported.

[Milestone fulfilled. An SOEC cell, which was tested at 850 °C and -1.5 A/cm² for 900 h, was selected for the study. 3D reconstruction and microstructure analysis was conducted on the Ni/YSZ electrode along the hydrogen/steam flow direction at four different locations. A degradation model was proposed in correlation with the current distribution.]

M1.3 MTC based SOEC cells using environmentally friendly organics for production with an initial performance of reaching a current density of 1.5 A/cm² below thermoneutral voltage at 750 °C demonstrated.

[Milestone fulfilled. Most tape-casting recipes contain toxic and environmentally unfriendly substances such as phthalates. We replaced phthalate with a new environmentally friendly plasticizer identified in the current project and implemented in all tape-cast layers (support, active fuel electrode, electrolyte and barrier layer). The cells produced following the above route reached the target performance.]

M1.4 Optimized SOEC cells tested at or close to thermoneutral voltage over a period exceeding 6 months, demonstrating a degradation rate of less than 0.5 %/1000 h at 1.25 A/cm².

[Milestone partially fulfilled. The SOEC cell durability at -1.25 A/cm² was significantly enhanced and the most successful route turned out to be infiltrating CGO ((Ce,Gd)O_{2-δ}) electrocatalysts into the Ni/YSZ electrode. A single cell test has been run for >6000 h. The cell degradation was reduced by a factor of 15 from 714 mV (60 %)/1000 h for the reference cell to 50 mV (4 %)/1000 h for the improved cell.]

- M1.5 Fuel electrodes with enhanced carbon tolerance tested at the cell level within the thermodynamic regions for coke formation over a period exceeding 500 hours, with a degradation rate of less than half that of the Ni/YSZ electrode demonstrated.
[Milestone fulfilled. We developed an SOEC cell with a Ni-free fuel electrode. The cell was exposed to carbon deposition inducing condition. The Ni-free fuel electrode was completely stable, showing no sign of carbon deposition. For comparison, a Ni/YSZ supported SOEC cell was tested under similar conditions and degraded and coked as expected.]
- M2.1 Coated ICs or IC alloys tested in reducing atmospheres resembling the fuel side environment of SOEC stacks over a period exceeding 2000 h with a corrosion rate constant less than $2 \times 10^{-14} \text{ g}^2 \text{ cm}^{-4} \text{ s}^{-1}$ demonstrated. (Month 12)
[Milestone fulfilled. We conducted corrosion tests of uncoated and coated Crofer 22 APU in H₂O/H₂ (90/10) at 750 °C for 2000 h. Among the coated samples, Y-coated ones showed the lowest corrosion rate of $0.2 \times 10^{-14} \text{ g}^2 \text{ cm}^{-4} \text{ s}^{-1}$ (evaluated from mass gain).]
- M2.2 ICs or IC alloys coated with improved EPD coating tested in oxygen over a period exceeding 4000 h with a corrosion rate constant less than $1 \times 10^{-14} \text{ g}^2 \text{ cm}^{-4} \text{ s}^{-1}$ demonstrated. (Month 18)
[Milestone partially fulfilled. We conducted long term testing of coated Crofer 22 APU at 800 °C in both air and oxygen atmospheres for more than 4000 h. Y+MCO dual layer coated samples showed the lowest corrosion rate of $1.57 \times 10^{-14} \text{ g}^2 \text{ cm}^{-4} \text{ s}^{-1}$ in pure oxygen.]
- M2.3 Testing of ICs with the best coatings developed in this project over a period >8000 h carried out and prediction of IC life-time under typical electrolysis operation conditions reported.
[Milestone partially fulfilled. The oxidation behaviour of large ICs with various coatings was investigated at 800 °C in air for periods up to 7000 h and the oxidation tests are still continuing. The lifetime of coated ICs was predicted based on the oxidation rate constant of coated Crofer 22 APU.]
- ~~M2.4 Optimized end-plate braze IC joint tested at 1 A/cm^2 over a period >1000 h, with 50 % reduction in the degradation rate of interface resistance as compared to the standard joint in the 2014 generation SOEC stacks demonstrated.~~
[Milestone replaced by M2.6. The milestone M2.4 in WT2.2 was formulated based on the old HTAS stack design (Delta), where the described interface "end-plate-braze-IC joint" was problematic. This problem was however resolved already after introducing the new HTAS stack design (TSP-1). M2.4 hence became irrelevant and was replaced by M2.6.]
- M2.5 Limits of operating conditions with regard to free of contact loss for the 2014 generation SOEC IC-cell interface identified.
[Milestone fulfilled. The oxygen electrode-IC interface was considered (by all stakeholders) as one of the weakest interfaces in the 2014 generation SOEC stacks. We carried out both experimental characterization of interface adherence and computer simulation of stresses. The peeling stress at the IC-cell interface was calculated and the occurrence of contact loss was estimated. Limits of operating conditions with regard to free of contact loss were proposed.]
- M2.6 Optimized oxygen electrode to IC joint developed, with 50 % improvement in terms of interface fracture toughness at the critical interface compared to the standard joint in the 2014 generation SOEC stacks demonstrated.
[Milestone fulfilled. By replacing the standard contact component at the oxygen electrode – IC joint with a CuMn foam, we increased the interface fracture energy by a factor of >2.]
- M3.1 Two stack tests for evaluating reliability of the 2014 generation SOEC stacks through different transient modes (SOEC/SOFC or SOEC/OCV etc.) including both load and possible temperature cycles for a period exceeding 1000 h completed.
[Milestone fulfilled. Two stacks were tested, one (U-052) through different transient modes including both load and temperature cycles and the other (X-045) simulating 100 % wind power absorbing. Both tests were run for 2000 h.]
- M3.2 Two stack tests to investigate stack degradation under different operating temperature and/or different voltages for a period exceeding 1000 h carried out.
[Milestone fulfilled. We tested two stacks (X-088 and X-075) under CO₂ electrolysis conditions at - 63 A and 25 % conversion, but at different temperatures (700 and 800 °C) to evaluate the effect of temperature on stack performance and durability. The total testing period exceeded 13,000 h.]

- M3.3 Two stack tests to investigate limits of stack operation with regard to possible stack operating parameters such as feed gas stream composition, conversion rate for steam/CO₂, current density etc. over a period exceeding 1000 h completed.
[Milestone fulfilled. Three stacks were tested. Stack K-755 was tested for co-electrolysis of steam and CO₂ at different temperatures and current densities for 6000 h. Stack Q-657 was tested for CO₂ electrolysis for 3000 h to investigate effect of gas impurities on stack degradation. Stack U-053 was tested also for CO₂ electrolysis for 500 h to investigate stack degradation at high current density.]
- M3.4 Life-time prediction of the 2014 generation SOEC stacks under representative SOEC operation schemes reported.
[Milestone fulfilled. It is concluded that the TSP-1 stacks (as per 2014 generation) will have a life-time of at least one year and there are indications on lifetime exceeding two years.]
- M3.5 Three stack tests of SOEC stacks composed of improved cells or stack components or with optimized operation strategy for a period exceeding 500 hours completed.
[Milestone partially fulfilled. Two stacks (U-052 and X-131) were tested with a total period exceeding 2600 h. Stack X-131 was one of the first stacks with improved gas flow distribution, while Stack U-052 incorporated both the improved flow distribution and a new contact layer for the oxygen electrode side.]
- M3.6 One SOEC stack test under optimum electrolysis conditions for a period exceeding one year with an ASR of less than 0.40 Ω cm² and an average degradation rate of less than 1 %/1000 h at 1 A/cm² demonstrated.
[Milestone partially fulfilled. Three stack tests (X-088, X-078, X-076) were devoted to M3.6, with a total testing period exceeding 17,000 h. Stack X-088 was tested at 700 °C and -63 A for 10,400 h. Taking the whole test into account the total degradation ended up being approximately 20 mV (1.4 %) /1000 h.]
- M4.1 Implications of the Danish power grid and power electronics on SOEC stacks identified and technical requirements for stack operation (in terms of voltage/current density/temperature, response time, cycling rate for transient operation etc.) reported.
[Milestone fulfilled. This milestone was accomplished by a literature review on electrolyser participation in electricity markets with both transmission- and distribution-level applications, an analysis of optimal size, voltage level, and participating strategy of electrolysers, and proposed scenarios regarding deployment of electrolysers in the Danish electricity grid.]
- M4.2 Schematic designs of future SOEC plants for at least two application scenarios (e.g. reversible SOEC/SOFC operation for grid balancing, SOEC enabled syngas production, or SOEC enabled synthetic fuel production etc.) established.
[Milestone fulfilled. Two application scenarios were investigated, one on SOEC steam electrolysis for hydrogen production and the other on reversible SOC plant for full energy system balancing. The corresponding SOEC plants were established.]
- ~~M4.3 Performance of a brazed 14x14x3 cm³ heater tested.~~
- ~~M4.4 Performance of a SOEC-CORE system with a brazed heater tested.~~
[Replaced with new milestones. Due to introduction of the new TSP-1 stack design, the activities on electrical heaters no longer reflected the actual need at HTAS for further stack technology development. Modifications to WT4.2 including M4.3 and M4.4 were proposed.]
- M4.3 Temperature profiles of a SOEC-CORE system in operation acquired and compared with model simulations.
[Milestone fulfilled. A specific test was set up with 2 TSP-1 stacks tested in a SOEC-CORE, with one of the stacks equipped with 16 additional thermocouples on the surface of the stack casing. The casing surface temperature was measured at various operating points and was further compared with the COMSOL stack model.]
- M4.4 Performance of an enhanced SOEC-CORE system tested.
[Milestone fulfilled. An improved SOEC-CORE system (with respect to improved heat distribution, lower pressure drops across components etc.) was developed and constructed within this project. The test results confirmed improved thermal insulation of the new CORE design.]
- M4.5 Performance of a reversible power supply unit integrated with a 10 kW SOEC-CORE system tested.
[Milestone partially fulfilled. We developed a novel PCU architecture and based on that two types of DC-DC converters: a three-phase interleaved Boost converter (IBC, 4 kW) and a dual-active-

bridge (DAB, 5 kW) converter. Due to the complexity of the SOEC-CORE system, the integration of the designed converter into the 10 kW SOEC-CORE system was not realized in this project. However, the DAB converter has demonstrated a maximum efficiency of 96.5 % and its control has been tested with a real 14-cell SOC stack, showing promising results and potential in integration into SOEC-CORE systems in future projects.]

M5.1 Results of the assessment of the role of electrolyzers on electricity markets towards 2020 (short-term) and 2020-2035 (long-term) in an international energy market context reported.

[Milestone fulfilled. The results were summarized into a public report. It is concluded that the role of electrolysis should be primarily for electrofuel production, as it can provide the missing link between intermittent renewable energy, resource scarcity and dependence on high-density fuels.]

M5.2 Danish roadmap for large-scale implementation of electrolyzers for the period 2020-2035 established.

[Milestone fulfilled. The roadmap was created based on the stakeholders input, previous studies, technology status and literature review and was divided into four main stages: Phase 1 Market preparation – from now to 2020, Phase 2 Market uptake – from 2020 to 2025, Phase 3 Market implementation – from 2025 to 2035, and Phase 4 Large scale implementation in smart energy systems – from 2035 onwards. The roadmap further looked into different activities, measures and incentives that should be implemented in order to speed up and maximize the implementation of electrolysis. The results were summarized into a public report.]

M5.3 Coherent technology data sheets for energy system analyses for the production of synthetic fuels for the transport sector established.

[Milestone fulfilled. The pathways to produce methane, methanol, DME (dimethyl ether) and kerosene (jet fuel) were analysed. The involved technologies and their development status were reviewed, including electrolysis (alkaline, PEM and SOEC), biogas plants, thermal gasification, carbon capture, and fuel synthesis. The potential of these technologies and the overall investment costs were assessed. The full analysis will be published into a public report.]

1.5.2 WP1 – Cell development and testing

WP1 focused on the SOEC cell level. It involved the following tasks:

- experimentally evaluating lifetime performance of the 2014 generation SOEC cells and exploring lifetime limiting factors
- continuing to further understanding of degradation mechanisms
- and based on the acquired knowledge finding out counter-acting measures and developing SOEC cells with enhanced durability and enhanced carbon tolerance.

These tasks were conducted by DTU Energy mainly.

1.5.2.1 WT1.1 – Grid balancing related single cell testing

In this project we have carried out both single cell and stack testing using the same grid balancing scheme, simulating 100 % absorption of wind power. The stack test results will be presented in Section 1.5.4 of this report. Here only the cell test results are presented. In collaboration with Senior Scientist Yi Zong from DTU Elektro, we looked into wind power production in the Danish island Bornholm. The Bornholm power distribution system is part of the Nordic interconnected system and fully integrated in the power market "DK2". It is located at the Danish island of Bornholm in the Baltic Sea, and is connected to the Swedish main grid via a sea cable (see Figure 1a). The system comprises about 28,000 electricity customers (55 MW peak load) and has very high penetration of a variety of low-carbon energy resources, including wind power (30 MW), CHP (16 MW), Photo Voltaic (1 MW), active demands and electric vehicles. Attempt is currently made to further increase the amount of renewable energy resources, especially wind power as well as storage. There are totally 4 wind farms in Bornholm and the data analyzed in this report is one of the four wind farms. Figure 1b presents the yearly wind power generation of the selected wind farm. The recorded data have a resolution of 5 minutes. The maximum power output was 12.5 MW. The average was 2.8 MW, equivalent to 22.14 % of the maximum power output.

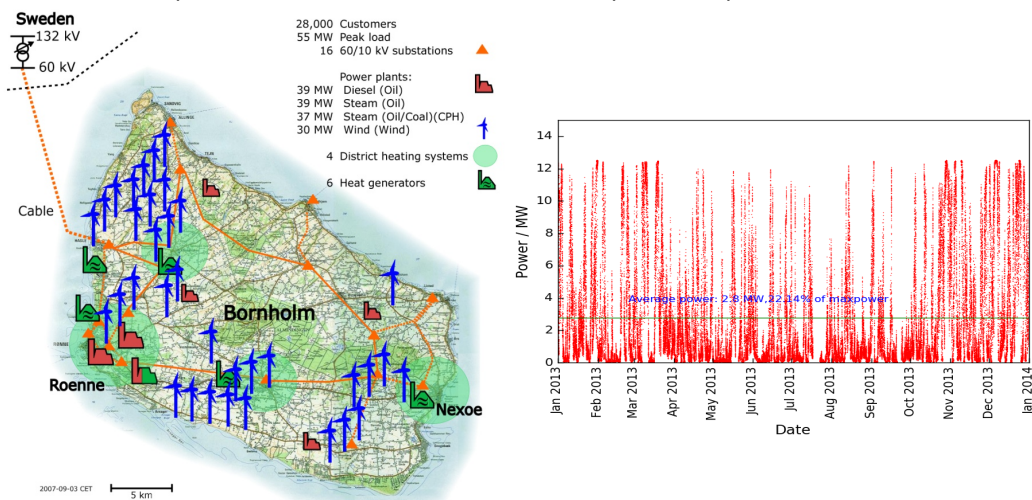


Figure 1: Illustration of the Bornholm power distribution system and overview of the wind power generation for the entire year 2013.

Within the 2013 year, the month July shows the lowest wind power generation and the month December shows the highest. For SOEC single cell testing, the recorded wind power data were scaled down with a factor of 1/980, assuming that the SOEC cell has an area specific resistance (ASR) of $0.24 \Omega \text{ cm}^2$ (when fed with 10 % H_2 + 90 % H_2O to the Ni/YSZ electrode at 800 °C) and that the maximum current density is -0.75 A/cm^2 . In the actual single cell testing, the month December data was employed to design an operating profile simulating 100 % absorption of the wind power by SOEC. Figure 2 presents the simulated single cell test profile and the actual recorded data for the entire December month. The single cell test demonstrates that SOEC can follow the wind power generation at a resolution of 5 minutes quite well.

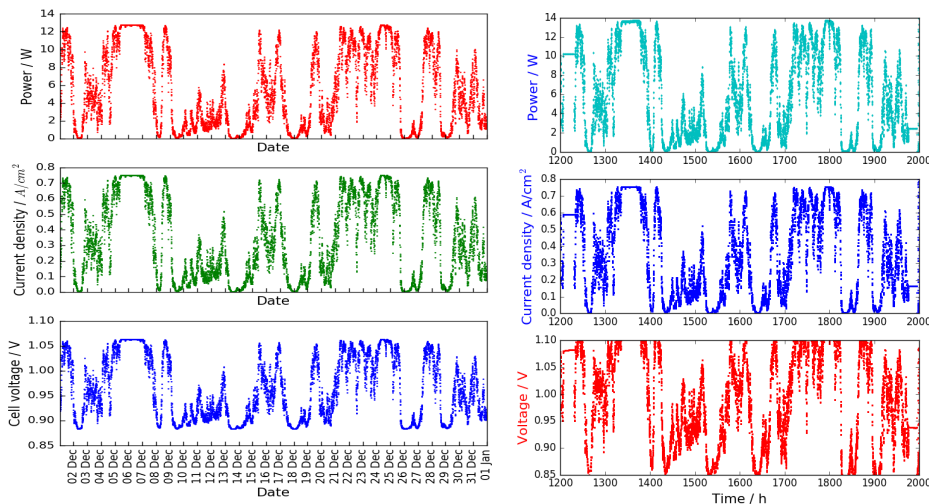


Figure 2: Simulated single cell test profile (left) and the actual recorded data (right) based on 100 % absorption of the wind power.

The wind profile run seem having not introduced any additional degradation. This is further supported by the stack test results (will be presented in Section 1.5.4 of this report). The longest SOEC single cell test completed in this project has reached 9000 h steady state electrolysis operation (Section 1.5.2.2), whereas the longest record for stack testing is 10,400 h (Section 1.5.4). It can be concluded that the lifetime of the 2014 generation SOEC cells is beyond one year and there are indications on lifetime exceeding 2 years. This consideration on lifetime does not take into account the improvements to the SOEC cells achieved in this project. **The milestone M1.1** (*M1.1 Life-time of the 2014 generation SOEC cells under the representative SOEC operation schemes identified in WT4.1 (which fulfils the technical requirements for the Danish power grid for grid balancing) predicted*) **is fulfilled**.

1.5.2.2 WT.1.2 – Advanced 3D structure characterization

At high current density (equal to or above -1 A/cm^2), SOEC electrodes degraded significantly with time. It is frequently seen that the Ni phase in Ni/YSZ electrodes suffers the most from structural changes. At high current density and high fuel utilization there is a large difference in microstructure evolution from the fuel inlet to outlet. In this project, we applied 3D characterization to investigate Ni/YSZ electrode microstructure evolution along the fuel flow direction in long-term tested SOEC cells. The SOEC Ni/YSZ electrode selected for 3D microstructure characterization is from a single repeating unit cell test reported previously.² The cell was run for 900 h at $850 \text{ }^\circ\text{C}$ and -1.5 A/cm^2 with 24 l/h 50 % H_2 + 50 % H_2O supplied to the hydrogen electrode compartment. The sample was previously characterized in terms of electrochemical performance and SEM and TEM studies. These initial studies showed a severely degraded microstructure dependent on the location of the observed site relative to the gas inlet and outlet. 3D image data were collected at 4 sites in the Ni/YSZ electrode: fuel gas inlet, gas outlet, center and under the glass sealing. The sample from under the glass sealing was included as an internal reference since this site has experienced the same temperature and atmosphere but no current. 3D data were collected by focused ion beam (FIB) serial sectioning on a Zeiss 1540 XB microscope. The four sites were compared in terms of simple microstructure parameters, such as phase fraction, interface area, percolating triple phase boundary (TPB) etc. The obtained 3D microstructure data were employed to further calculate tortuosity factor, TPB tortuosity, and critical pathways. The main findings from the analyses are summarized below:

- A severe reduction in the quality of the transport network was observed for the center and inlet sites. This is characterized by a significantly lower fraction of percolating TPB sites mainly caused by a reduction in Ni phase percolation and a significantly

² Sun, X., Chen, M., Liu, Y.L., Hendriksen, P.V. and Mogensen, M., 2013. Durability of Solid Oxide Electrolysis Cell and Interconnects for Steam Electrolysis. *ECS Transactions*, **57(1)**, pp.3229-3238.

higher tortuosity factor due to both longer transport pathways and narrow bottle-necks.

- It is interesting to observe that the outlet site has transport network properties very similar to the reference site indicating that only very limited current-related degradation has taken place.
- Of similar interest is the fact that the reference site Ni network has degraded almost as much as the outlet site.
- These observations support a degradation model that starts at the inlet and then spreads as a front across the cell towards the outlet as the active sites at the inlet suffer from increasingly degraded Ni transport networks.

The milestone M1.2 (3D reconstruction and microstructure analysis of long-term tested SOEC electrodes and corresponding reference carried out and quantitative 3D descriptions reported) is achieved.

1.5.2.3 WT1.3 – Optimized SOEC cells with enhanced durability

WT1.3 was to continue the efforts launched in the previous project (ForskEL 12013) on Ni/YSZ supported SOEC cells and use various measures to further improve the durability at current density equal to or above -1.25 A/cm^2 . In ForskEL 12013, we have developed one type of Ni/YSZ supported SOEC cells and tested at $800 \text{ }^\circ\text{C}$ and -1 A/cm^2 . The test was conducted for 2000 h and the cell showed very low degradation rate (0.3-0.4 %/1000 h). A reproduction of this cell was conducted in the current project (ForskEL 12276). Single cell test of this “reproduction-cell” shows that the cell has an initial performance identical to that of the previous and world-record-breaking cell. However the reproduction cell experienced a slightly higher degradation. The long-term test was continued for up to a one-year, making it the longest running SOEC test in Denmark. The development of cell voltage, polarization resistance and ohmic resistance is depicted in Figure 3.

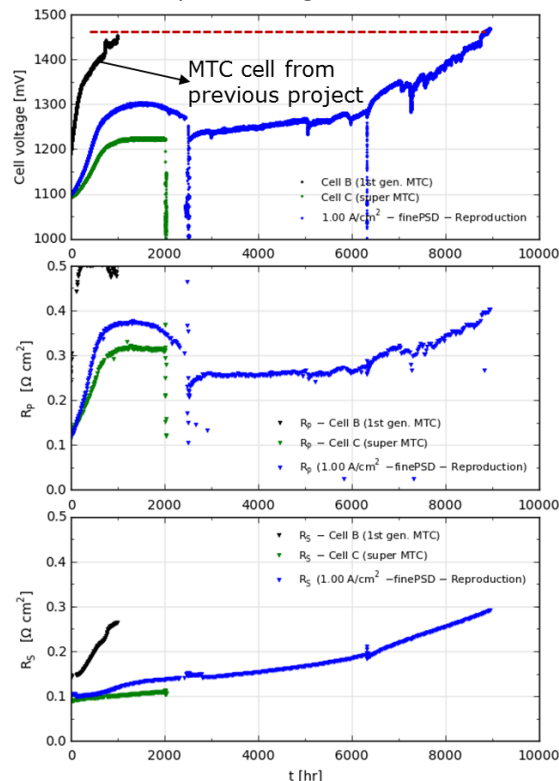


Figure 3: One-year SOEC single cell test conducted in the current project (ForskEL 12276). Development of cell voltage, polarization resistances (R_p) and ohmic resistance (R_s) for the microstructure optimized MTC cell with a Ni/YSZ:40/60 ratio (green curves, test conducted in ForskEL 12013) and the re-production of this fuel electrode (blue curves). Galvanostatic tests were operated at $800 \text{ }^\circ\text{C}$, oxygen to the oxygen electrode, 90 % H_2O in H_2 to the fuel electrode with a flow corresponding to a steam utilization of 56 % at -1 A/cm^2 .

There were several test-related “incidents” during the one-year test (e.g. power supply issues, repair of pO_2 -sensor during testing, gas-sensor break-down etc.) as evident from the plots of the raw data in Figure 3. During the first part of the test (0-1000 h) the main increase in R_p is due to impedance increase in the frequency range 100 Hz to 10 kHz indicating that it is mainly the fuel electrode that degrades. However it is also the fuel electrode that seems to activate from approximately 1200 to 2200 h of testing (frequency range 500 Hz to 2 kHz for the decreasing impedance response), while the ending degradation from app. 7 kh to 9 kh of testing is caused by an increase in impedance in the frequency range from app. 10 Hz to 10 kHz indicating that it can be both electrodes that degrade.

In the current project, the microstructure optimization still focused on the Ni/YSZ fuel electrode and was based on the processing details and microstructure requirements described in a patent application³. One of the development targets in WT1.3 was towards environmentally friendly production of SOEC. Active layers for SOEC cells are produced by multilayer tape-casting, where a suspension of the ceramic material (NiO and YSZ) is dispersed in a solvent and the particle size is afterwards reduced by ball milling. To obtain the right processing behavior an organic binder and plasticizer have to be added, when the optimal particle size of the ceramics in the suspension is obtained. Most tape-casting recipes contain toxic and environmentally unfriendly substances such as phthalates and strong lipophilic solvents. It is therefore necessary to pay attention to substitute these hazard substances if the fabrication of SOEC cells is to be turned into upscaled production. In the current project, the first priority has been to substitute the phthalates to less hazard generations of plasticizers. The polymer industry has strong focus on these topics and is continuously developing new more efficient and less toxic plasticizers. A systematic screening of these new plasticizers has been carried out and a promising candidate was found. The identified substance is a Polyoxyethylen aryl ether and is not included in the European Chemicals Agency’s “Candidate list of substances of very high concern for authorization”. The new environmentally friendly plasticizer was then implemented in all tape-cast layers (support, active fuel electrode, electrolyte and barrier-layer). Besides the environmental benefit, improved process ability was obtained for the multilayer tape-cast process where a better dispersion of the adhesion between electrolyte and barrier layer was obtained. One of the cells produced following the above route was characterized at 750 °C. This cell reached thermoneutral potential at -1.5 A/cm^2 when applying a fuel mixture of $p(H_2O)/p(H_2)$ of 90/10. Figure 4 shows SEM of the as-produced non-reduced cell and the iV-curve fulfilling the performance goal in M1.3. **With this M1.3 (MTC based SOEC cells using environmentally friendly organics for production with an initial performance of reaching a current density of 1.5 A/cm^2 below thermoneutral voltage at 750 °C demonstrated) is fulfilled.**

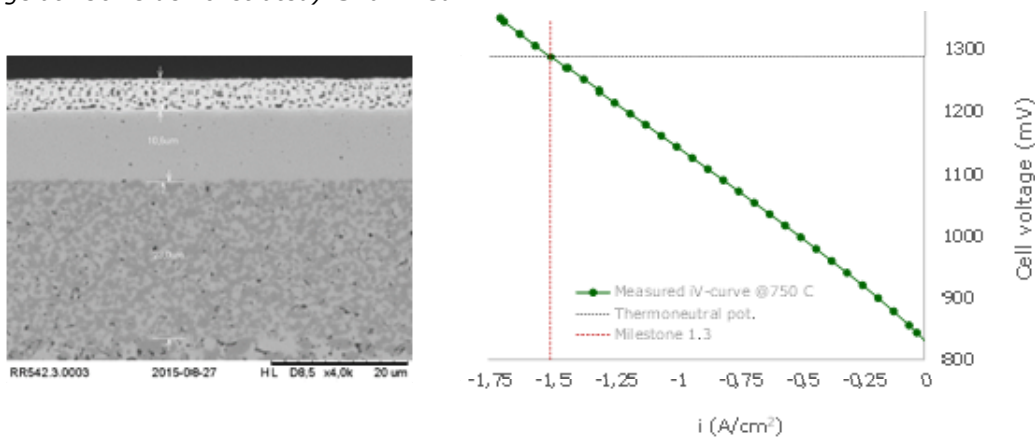


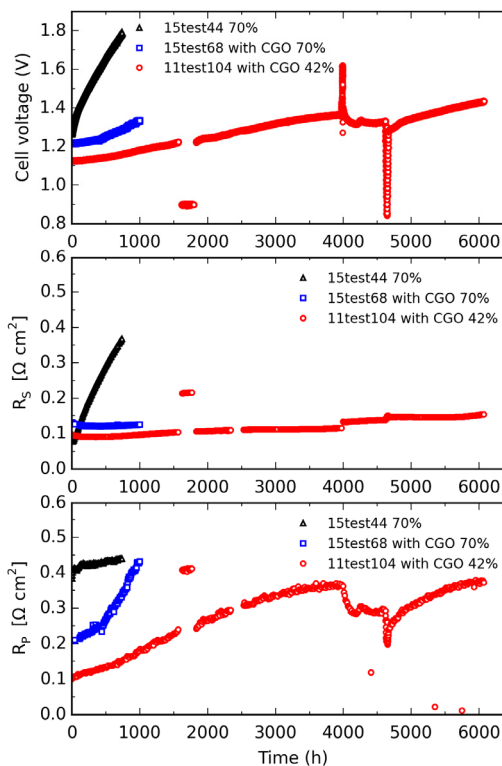
Figure 4: SEM image for fuel electrode, electrolyte and barrier layer prior to addition of oxygen electrode and reduction (left). This cell was used for the iV-curve (right) at 750 °C and applying a fuel mixture of $p(H_2O)/p(H_2)$ of 90/10.

³ K. Brodersen, A. Hauch, M. Chen, J. Hjelm, Durable Fuel Electrode, Patent application no Ep15181381.3, 2015.

The second task of WT1.3 was to improve cell durability at current density equal to or above -1.25 A/cm^2 . The 2014 generation SOEC cells showed severe degradation when tested at these conditions and the Ni/YSZ electrode was identified as the main cause of the degradation. In order to reduce the degradation and to extend the cell lifetime, various efforts were devoted to optimizing Ni/YSZ electrode microstructure. The most successful route turned out to be introducing CGO catalysts into the Ni/YSZ electrode. As shown in Figure 5, the 2014 generation SOEC cells showed a degradation rate of $714 \text{ mV}/1000 \text{ h}$ (or $60 \text{ \%}/1000 \text{ h}$) at -1.25 A/cm^2 with 70 \% steam conversion. The cell degradation was dominated by huge R_s increase. With CGO catalysts, the degradation rate was reduced to 117 mV (10 \%) and 50 mV (4 \%)/ 1000 h at 70 \% and 42 \% conversion, respectively. The degradation was dominated by the increase in R_p , which tended to flatten out with time as shown in Figure 5. According to impedance analysis, the huge improvement was due to the resistance decrease for the electrochemical reactions happening at the Ni/YSZ electrode TPB, where CGO was believed to play an important role. The test 11test104 has been run for more than 6000 h at -1.25 A/cm^2 and is still performing OK though experienced several test related incidents.

Figure 5: Galvanostatic long-term steam electrolysis durability tests under -1.25 A/cm^2 at $800 \text{ }^\circ\text{C}$. a) Voltage development during time, b) ohmic resistance and c) polarization resistance development during time (extracted from EIS). The test 15test44 was conducted in ForskEL 12013 on 2014 generation SOEC cells, while the tests 15test68 and 11test104 were carried out in ForskEL 12276 where CGO was introduced into the active Ni/YSZ electrode. Different steam conversion was employed in these tests: 70 \% for 15test44 and 15test68 and 42 \% for 11test104. The degradation rate was calculated based on the test data over the entire test period for all the three tests.

As demonstrated above, we have made a significant achievement in improving the cell durability at -1.25 A/cm^2 , bring down the cell degradation by a factor of 15 from 714 mV (60 \%) / 1000 h to 50 mV (4 \%)/ 1000 h . **The milestone M1.5 (Optimized SOEC cells tested at or close to thermoneutral voltage over a period exceeding 6 months, demonstrating a degradation rate of less than $0.5 \text{ \%}/1000 \text{ h}$ at 1.25 A/cm^2) is considered partially fulfilled.**



1.5.2.4 WT1.4 – Optimized SOEC cells with enhanced carbon tolerance

The aim of WT1.4 was to develop SOEC fuel electrode with enhanced carbon tolerance dedicated for electrolysis of CO_2 or co-electrolysis of steam and CO_2 . Previous strategies for avoiding destructive carbon formation for a standard Ni/YSZ supported SOEC cell include tailoring the operating conditions⁴, modifying the Ni/YSZ electrode by infiltration of CGO⁴, and alloying the Ni/YSZ electrode with Al_2O_3 . However, with Ni present in the fuel electrode, it will not be possible to surpass the Boudouard threshold of carbon deposition that severely limits the reactant gas conversion.

We first tested a Ni/YSZ cell as a reference. Figure 6a compares the ohmic resistances (R_s), polarization resistances (R_p) and OCV of the cell before and after coking in $p\text{CO}:p\text{CO}_2$

⁴ Skafte, T. L., Graves, C., Blennow, P., & Hjelm, J., "Carbon Deposition during CO_2 Electrolysis in Ni-Based Solid-Oxide-Cell Electrodes", ECS Transactions, 68, 3429–3437 (2015).

0.89:0.11, measured at 756 °C with $p_{H_2}:p_{H_2O} = 0.96:0.04$ on the fuel side and dry air on the oxygen side. Note that the theoretical carbon deposition threshold is $p_{CO}:p_{CO_2} = 0.794:0.206$ at 756 °C. The R_s increased from $0.34 \Omega \text{ cm}^2$ initially to $0.91 \Omega \text{ cm}^2$ after coking; a factor of 2 increase. Total area-specific resistance (ASR) increased from $1.02 \Omega \text{ cm}^2$ to $1.65 \Omega \text{ cm}^2$, a 62 % ASR increase. Furthermore, the OCV decreased from 1084 mV to 1058 mV in $H_2:H_2O = 0.96:0.04$ (theoretical: 1096 mV). Carbon residue and small cracks were observed when investigating the cell after testing, as seen in Figure 6b. The electrode surface at the inlet was covered with carbon while the outlet showed less carbon residue as air had presumably leaked through the electrolyte and oxidized the carbon. These observations suggest that the cracking of the cell can be ascribed to the damage caused by carbon formation and subsequent carbon oxidation upon changing back to $p_{H_2}:p_{H_2O} = 0.96:0.04$.

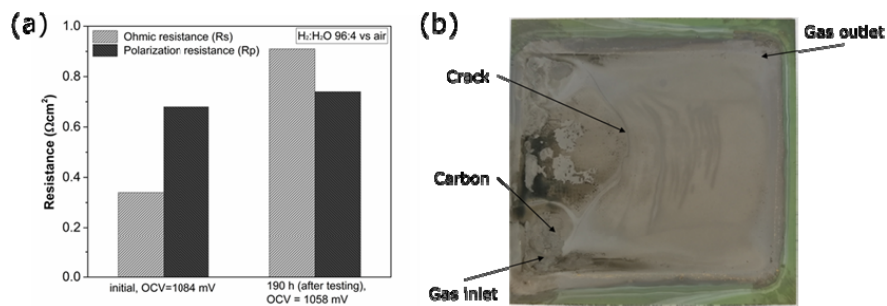


Figure 6: (a) Ohmic resistance, polarization resistance and OCV data of a Ni/YSZ supported SOEC cell before and after carbon deposition, measured at 756 °C with $p_{H_2}:p_{H_2O} = 0.96:0.04$ to the fuel electrode and dry air to the oxygen electrode. (b) A photo of the cell after testing.

To avoid carbon deposition, a cell with a Ni-free fuel electrode was fabricated, partially based on previous cell development work at the department⁵. The cell had the structure illustrated in Figure 7. As seen in Figure 7b, the cell did not degrade significantly during 550 h of carbon deposition inducing conditions ($p_{CO}:p_{CO_2} = 0.84:0.16$, 750 °C). Note that the carbon deposition threshold is $p_{CO}:p_{CO_2} = 0.777:0.223$ at 750 °C. R_s remained stable, only increasing from $0.81 \Omega \text{ cm}^2$ to $0.83 \Omega \text{ cm}^2$, measured in $H_2:H_2O = 0.80:0.20$. R_p increased from $0.51 \Omega \text{ cm}^2$ to $0.62 \Omega \text{ cm}^2$, but from investigation of the impedance data it is clear that the degradation originated entirely from the oxygen electrode, while the fuel electrode was completely stable. The total ASR increased from $1.32 \Omega \text{ cm}^2$ to $1.45 \Omega \text{ cm}^2$, i.e. a 10% ASR increase. The OCV decreased slightly from 1000 mV to 993 mV in $H_2:H_2O = 0.80:0.20$ (theoretical: 1018 mV), likely due to minor pinholes in the thin electrolyte. Thus, no signs of carbon deposition was observed, and it is concluded that the new cell is carbon deposition tolerant and **the milestone M1.5 (Fuel electrodes with enhanced carbon tolerance tested at the cell level within the thermodynamic regions for coke formation over a period exceeding 500 hours, with a degradation rate of less than half that of the Ni/YSZ electrode demonstrated) is hereby accomplished.**

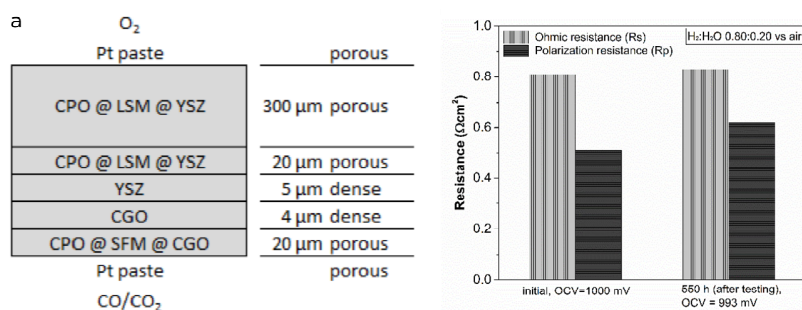


Figure 7: (a) Structure of the Ni-free cell. (b) Ohmic resistance, polarization resistance and OCV data before and after 550 h exposing to carbon deposition inducing conditions.

⁵ Skafte, T. L., Sudireddy, B. R., Blennow, P., & Graves, C., "Carbon and Redox Tolerant Infiltrated Oxide Fuel-Electrodes for Solid Oxide Cells", ECS Transactions, 72(7), 201-214 (2016).

1.5.3 WP2 – Stack components and interfaces

WP2 focused on stack components and their interfaces. It involved two work tasks:

- To further develop durable and cheap interconnects (ICs)
- To further improve reliability and robustness of the stack component interfaces.

These tasks were conducted mainly by DTU Energy.

1.5.3.1 WT2.1 – Durable and cheap ICs

The first part of WT2.1 looked into IC corrosion in reducing atmospheres resembling the fuel side environment of SOEC stacks. In this study uncoated and coated Crofer 22 APU steel samples were subjected to oxidation in a high steam (90 % steam, 10% H₂) hydrogen electrode atmosphere at 750 °C. These conditions resemble a possible SOEC hydrogen electrode inlet feed (or SOFC outlet). The coated steel (all Crofer 22 APU) samples include:

- Ni plated steel (~10 µm in coating thickness)
- Co plated steel (~2 µm)
- CGO deposited by physical vapor deposition (PVD) (~2 µm)
- Y (yttrium) deposited by electrolytic deposition (~100 nm)

Samples prepared by electroplating (Ni, Co) have been obtained by outsourcing the plating procedure (performed by Sur-Tech A/S). CGO has been deposited also by an external supplier. Samples with Y coating have been produced at DTU Energy in a process developed in the previous and current project (electrolytic deposition).

The oxidation test has been conducted for up to 2000 h. Samples coated with Ni or Co showed some oxide scale spallation already after 250 hours and were hence removed from the experiment. This indicates that Ni or Co alone is not suitable as coating material in hydrogen atmospheres with high steam content. In comparison to the uncoated sample, both CGO and Y coated samples showed visibly lower weight gain. The weight gain for these 3 types of samples is plotted in Figure 8. SEM images of the samples after 2000 h oxidation are presented in Figure 9. Uncoated sample showed heavy corrosion and formation of mixed Fe-Cr oxide. CGO coated sample showed low weight gain but the coating was spalling off to a large extent. The best behavior was observed for Y coated samples. This sample showed the lowest weight gain and adherent thin oxide scale. The Y coating has not been yet optimized, and it is believed that it can be still improved in the future.

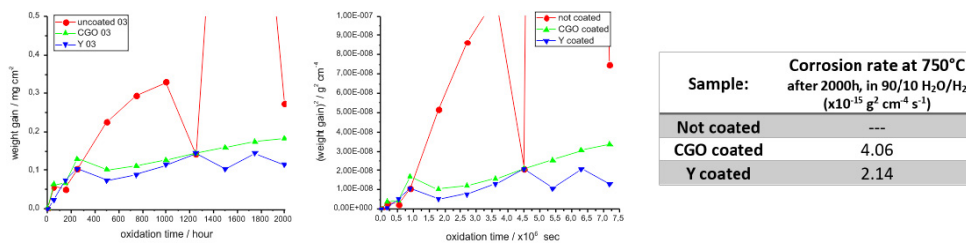


Figure 8: Linear and parabolic mass gain for uncoated, CGO and Y coated samples. In the table corrosion rate parameter is shown.

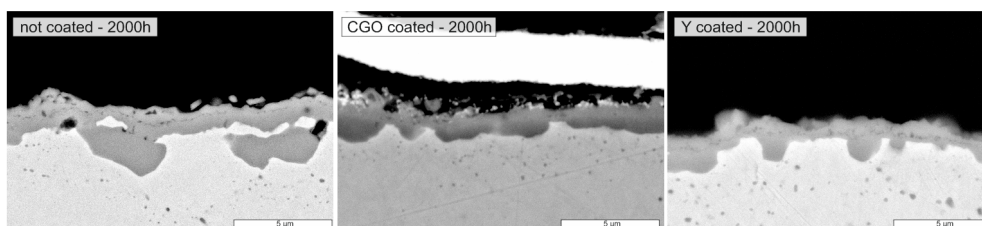


Figure 9: SEM cross section images of the samples oxidized for 2000 h.

With the results of Y coated samples, **the milestone M2.1** (Coated ICs or IC alloys tested in reducing atmospheres resembling the fuel side environment of SOEC stacks over a period exceeding 2000 h with a corrosion rate constant less than $2 \times 10^{-14} \text{ g}^2 \text{ cm}^{-4} \text{ s}^{-1}$ demonstrated) **is fulfilled**.

In the previous ForskEL project (ForskEL 12013), at DTU Energy, a ceramic coating based on $(\text{Co,Mn})_3\text{O}_4$ spinel has been successfully applied to the oxygen side of ICs using electrophoretic deposition (EPD). Within this project, the second part of WT2.1 was hence devoted to further optimization of the EPD coating process and implementation at the stack level, extended lifetime testing, and further enhancement of the corrosion resistance by applying a second layer coating (between the steel IC and the EPD spinel coating) using electrolytic deposition (ELD). We conducted long term testing of coated Crofer 22 APU alloys at 800 °C in both air and oxygen atmospheres. In total four types of samples were tested:

- Not-coated: reference samples;
- Y coated – thin (< 100 nm) reactive element coating (ELD);
- MCO coated - $\sim 20 \mu\text{m}$ $\text{Mn}_{1.5}\text{Co}_{1.5}\text{O}_4$ (EPD);
- Y+MCO – dual layer coating, a combined reactive element and spinel coating;

Coating microstructures are presented in Figure 10. The developed electrophoretic deposition method is compatible with the electrolytic deposition process. This allows for fabrication of dual layer coatings. These two processes also allow for coating large interconnect samples.

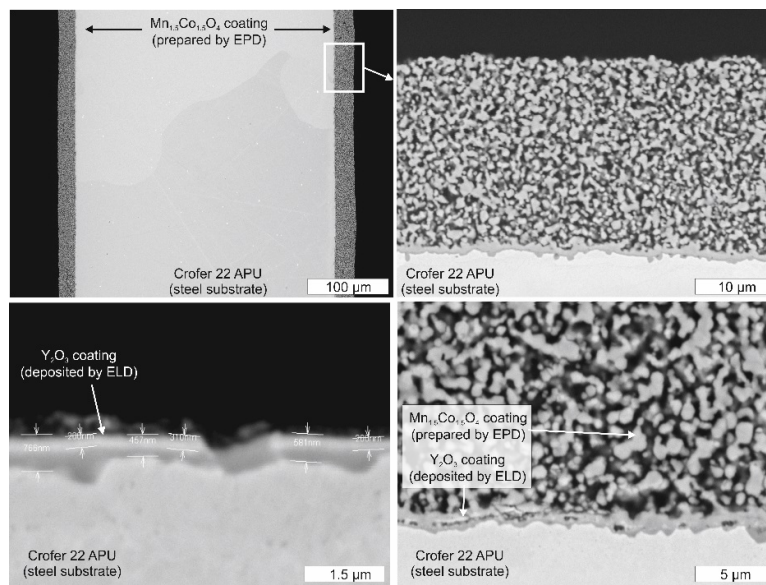


Figure 10: Cross section images of the developed coatings. A) Low magnification of the MCO sample, B) higher magnification of the MCO coating, C) Y coated sample, D) Y+MCO coated sample.

Table 1: Evaluated oxidation rate constants for the samples oxidized at 800 °C.

Sample type	Corrosion rate in air [$\times 10^{-14} \text{ g}^2 \text{ cm}^{-4} \text{ s}^{-1}$]	Corrosion rate in oxygen [$\times 10^{-14} \text{ g}^2 \text{ cm}^{-4} \text{ s}^{-1}$]	$k_{p(\text{ox})}/k_{p(\text{air})}$
Not-coated	6.51	12.7	1.95
Y	1.18	1.96	1.66
MCO	0.63	1.72	2.73
Y+MCO	0.52	1.57	3.02

The oxidation tests were carried out for more than 4000 h. Table 1 presents the oxidation rate constants evaluated from the mass gain. The corrosion rate of Crofer 22 APU was significantly reduced by the applied coating, for both in air and in oxygen. With the applied Y+MCO dual layer coating, a corrosion rate constant of $\sim 1.57 \times 10^{-14} \text{ g}^2 \text{ cm}^{-4} \text{ s}^{-1}$ in pure oxygen was achieved, which is very close to the project target. **The milestone M2.2** (ICs or IC alloys coated with improved EPD coating tested in oxygen over a period exceeding 4000 h

with a corrosion rate constant less than $1 \times 10^{-14} \text{ g}^2 \text{ cm}^{-4} \text{ s}^{-1}$ demonstrated) **is considered partially fulfilled.**

Within the project period, the EPD and ELD coating processes have also been up-scaled from the component level to the stack level. Coatings have been deposited on full scale shaped IC ($12 \times 12 \text{ cm}^2$). The oxidation tests were carried out in a chamber furnace in air at $800 \text{ }^\circ\text{C}$. Coated ICs employed in HTAS SOEC stacks were included in the study as reference. The tests have reached 7000 h at the end of this project and will be continued after reaching 10,000 h. Table 2 presents the oxidation rate constants evaluated from the measured mass gain. The values measured on large ICs ($12 \times 12 \text{ cm}^2$) are visibly higher than the ones on smaller samples ($2 \times 2 \text{ cm}^2$). The difference could be caused by temperature gradient inside the large chamber furnace used for the oxidation test of large coated ICs. But still, the corrosion resistance was significantly enhanced by the applied coatings.

Table 2: Oxidation rate constants of coated large ICs oxidized at $800 \text{ }^\circ\text{C}$ in air.

Sample type	Corrosion rate in air [$\times 10^{-14} \text{ g}^2 \text{ cm}^{-4} \text{ s}^{-1}$]	$k_{p(\text{IC})}/k_{p(\text{small-sample})}$
Not-coated	12.33	1.89
Reference	9.66	-
MCO	0.87	1.38
Y+MCO	0.72	1.38

Based on the long-term corrosion data, the lifetime of ICs was then calculated as time needed for depletion of Cr in the alloy to a level of 15 wt.%. Assuming a minimum thickness of the IC as $200 \text{ }\mu\text{m}$ and two representative corrosion rates ($2 \times 10^{-14} \text{ g}^2 \text{ cm}^{-4} \text{ s}^{-1}$ as a typical "safe" value for coated alloys and $6 \times 10^{-14} \text{ g}^2 \text{ cm}^{-4} \text{ s}^{-1}$ for uncoated alloys), calculated lifetime predictions are shown in Figure 11. Results are presented as a function of the initial alloy Cr content. Regarding alloys used in this study, Crofer 22 APU has 22-23 wt.% Cr, which is in the higher range for SOEC/SOFC alloys. Other cheaper alternative alloys (e.g. 430, 441) have lower Cr content and thus lowered protective element reservoir and will require shorter time to reach the 15 wt.% Cr limit. This simple model shows, that Crofer 22 APU alloy with the coating developed in this study will have a lifetime exceeding 60,000 hours assuming a corrosion rate of $2 \times 10^{-14} \text{ g}^2 \text{ cm}^{-4} \text{ s}^{-1}$ and above 100,000h with a corrosion rate of $1 \times 10^{-14} \text{ g}^2 \text{ cm}^{-4} \text{ s}^{-1}$, whereas the lifetime of not-coated alloy would be $< 20,000$ hours. **With the above results, the milestone M2.3 (Testing of ICs with the best coatings developed in this project over a period $> 8000 \text{ h}$ carried out and prediction of IC life-time under typical electrolysis operation conditions reported) is considered partially fulfilled.**

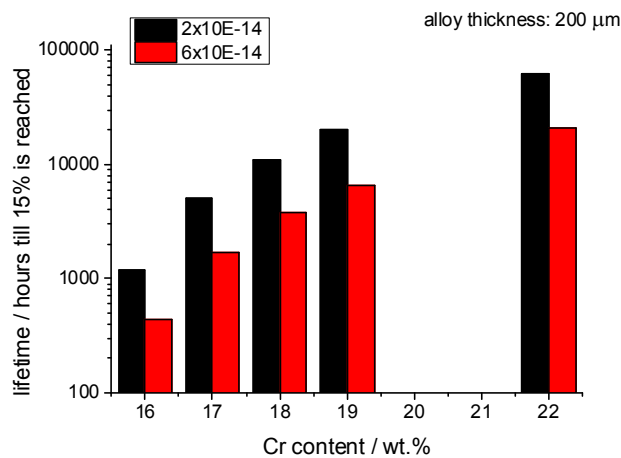


Figure 11: Expected lifetime of alloys with different Cr contents. Cases of not-coated and coated alloys are considered.

1.5.3.2 WT2.2 – Robust and reliable stack component interfaces

The performance and durability at the stack level is compromised by the weak contact or loss of contact between interconnects and cells. The purpose of WT2.2 was to characterize and analyze the interface adherence between the electrode and the IC under different configurations and conditions, to lay the foundation for improvement of interface adherence. Interface adherence is characterized fundamentally by the interfacial fracture toughness between the electrode and the IC. **The first part of WT2.2** was to identify operating conditions of SOEC such that contact loss between the interconnect and the cell can be avoided. Here we summarize measurement results on adherence of the critical interface involved in contact loss in the 2014 generation design, and then presents results of stress analysis corresponding to typical operating conditions. Recommendations on operating conditions for avoiding contact loss are made.

Interface adherence is characterized fundamentally by the interfacial fracture energy. Four-point bending of a notched bilayer was chosen for such measurement. The test configuration is shown in Figure 12. Four-point bending test was carried out at room temperature. The fractured interface indicates fracture occurs mostly between the Co-oxide layer and the LSM contact layer. The fracture energy measured for the interface is 1.0 N/m. This is comparable to the reported fracture toughness of 1.6 N/m for a similar interface - between MCO-coated 441 stainless steel and LSM. The methodology used for characterization and analysis is reliable.

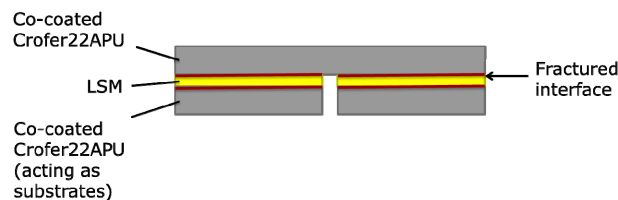


Figure 12: Sample configuration for interfacial fracture energy testing.

Further analysis at the stack level was done via computer simulation of stresses in a repeating unit consisting of an SOEC cell, a shaped IC, and sealing components. The cell components were assumed to behave elastically, while interconnects and sealing components had elastic and creep behavior. The peeling stress at the IC-cell interface was calculated and the occurrence of contact loss was estimated.

The main findings are summarized below:

- The two critical instants with highest peeling stresses during operation are immediately after temperature gradient is reached, and after cooling down to room temperature.
- The peeling stress reduces with the total creep rate of the interconnect. This is because materials with higher creep rate can relax stress faster.
- Thermal expansion coefficient mismatch has a significant contribution to the peeling stress at room temperature.
- Larger temperature gradient leads to higher peeling stresses.
- The compression force has a minor effect on peeling stress.
- Slower cooling speed is advantageous because more time is allowed for the materials to relax stress.
- An effective way to minimize peeling stress is through designing the micro-architectures of the interconnect.
- The peeling stress resulted from operation and cool down should be less than 1.5 kPa for the current interface of Co-coated Crofer 22 APU and LSM.
- The temperature gradient and the interconnect sheet thickness need to be reduced to lower the peeling stress occurring in the stack.

The milestone M2.5 (Limits of operating conditions with regard to free of contact loss for the 2014 generation SOEC IC-cell interface identified) **is fulfilled**.

The second part of WT2.2 focused on the adhesion between the LSC/CGO (LSC: $(La,Sr)CoO_{3-\delta}$) oxygen electrode, contact layers (CLs), the coated interconnects made of Crofer 22 APU. By measuring fracture toughness, we characterized the strength of the following interfaces: Co-coated Crofer 22 APU - CLs, MCO-coated Crofer 22 APU - CLs, and LSC/CGO oxygen electrode - CLs. The results were compared with the solution adopted in the 2014 generation SOEC stacks, where the LSM CL was screen printed onto the SOEC cell (the oxygen electrode side) to provide the bonding between the cell and the coated IC. In this project, four different types of contact layers were tested: $La_{0.6}Sr_{0.4}CoO_{3-\delta}$ (LSC), $(La_{0.8}Sr_{0.2})_{0.98}MnO_{3-\sigma}$ (LSM), LSC-LSM, and $LaNi_{0.6}Fe_{0.4}O_3$ (LNF). In addition, a CuMn foam was tried out to replace the ceramic contact layer. The measured fracture toughness (in term of fracture energy) is plotted in Figure 13. The conventional ceramic CLs have lower interface fracture energy both with the coated IC and with the oxygen electrode, being of approximately 1 J/m^2 . The CuMn-foam increased the interface fracture energy with the IC and O_2 electrode to 8.6 J/m^2 and 2.52 J/m^2 , respectively. The adhesion between the oxygen electrode and the coated IC was significantly enhanced by replacing the ceramic contact layer with the CuMn foam, as demonstrated in the current project.

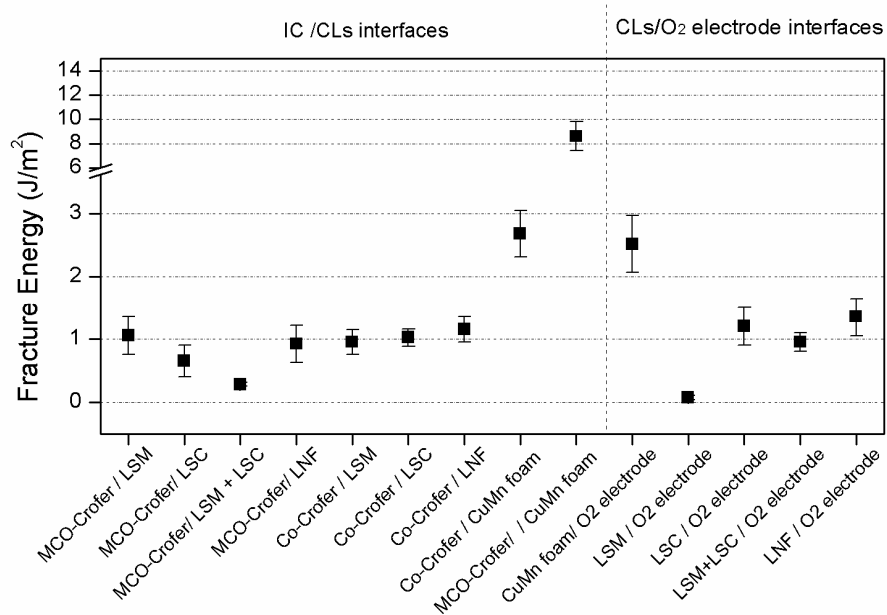


Figure 13: Fracture toughness results measured on different interfaces.

With the above results, **the milestone M2.6** (Optimized oxygen electrode to IC joint developed, with 50 % improvement in terms of interface fracture toughness at the critical interface compared to the standard joint in the 2014 generation SOEC stacks demonstrated) **is fulfilled.**

1.5.4 WP3 – Stack development and testing

The tasks in WP3 included identifying limiting conditions for the SOEC technology to absorb power fluctuations and getting closer experience with the benefit of utilizing the technology in reversible modes (i.e. SOEC/SOFC), while balancing the grid to renewable energy sources. These tasks were undertaken by both HTAS and DTU Energy. Table 3 gives an overview of stack testing in this project. In total we have carried out 10 stack tests under various conditions with a total testing period of 36,050 hours. The results obtained in WP3 are summarized below, grouped according to the work tasks.

Table 3: Overview of stack testing throughout the project.

Stack ID (number of cells)	Stack design	Milestone	Main purpose	Testing period, hour	Tester
U-052 (75)	TSP-1	M3.1, M3.5	Reliability through different transient modes + improved stack	2000	HTAS
X-045 (75)	TSP-1	M3.1	Wind profile test	2000	DTU Energy
X-075 (50)	TSP-1	M3.2	Degradation under different operating temperatures	3000	HTAS
X-088 (50)	TSP-1	M3.2, M3.6	Degradation under different operating temperatures + long term testing	10400	HTAS
K-755 (8)	Delta	M3.3	Limits of stack operation (current density)	6000	DTU Energy
Q-657 (8)	TSP-1	M3.3	Limits of stack operation (gas composition)	3000	DTU Energy
U-053 (75)	TSP-1	M3.3	Limits of stack operation (current density)	2000	HTAS
X-131 (75)	TSP-1	M3.5	Improved stack	600	HTAS
X-078 (50) ^a	TSP-1	M3.6	Long term testing (SOEC-CORE)	2700	HTAS
X-076 (50) ^a	TSP-1	M3.6	Long term testing (SOEC-CORE)	4350	HTAS

^a The tests were initiated at the end of the previous project (ForskEL 12013) and continued in the current project (ForskEL 12276).

1.5.4.1 WT3.1 – Grid balancing related stack testing

The first part of WT3.1 was devoted to evaluating reliability of the 2014 generation SOEC stacks through different transient modes (SOEC/SOFC or SOEC/OCV etc.) including both load and possible temperature cycles, to mimic different levels of grid balancing. Within the project period two stacks (U-052 and X-045) were tested for this purpose.

Stack U-052 was of the TSP-1 stack type design containing 75 cells with a foot print of 12x12 cm². The stack furthermore contained two different modifications and the results therefore contributed to the milestone M3.5 as well. The modifications are:

- Improved contact layer on the air side.
- Modifications to stack components to improve the internal gas distribution and flow field in the stack.

In order to evaluate the stack response to various transients, the following test program has been conducted:

- 1) Initial degradation testing for 500 h at -50 A, 30 % conversion, 750 °C, CO₂/H₂ (95/5 as input gas).
- 2) UI (voltage-current) test #1: 0 to -85 A, CO₂/H₂ (95/5).
- 3) 5 thermal cycles (TC) with 2 h testing at -50 A, 30 % conversion, 750 °C, CO₂/H₂ (95/5).
- 4) UI test #2: 0 to -85 A, CO₂/H₂ (95/5).
- 5) Change rig and testing for another 1500 h at -50 A, 30 % conversion, 750 °C, CO₂/H₂ (95/5).

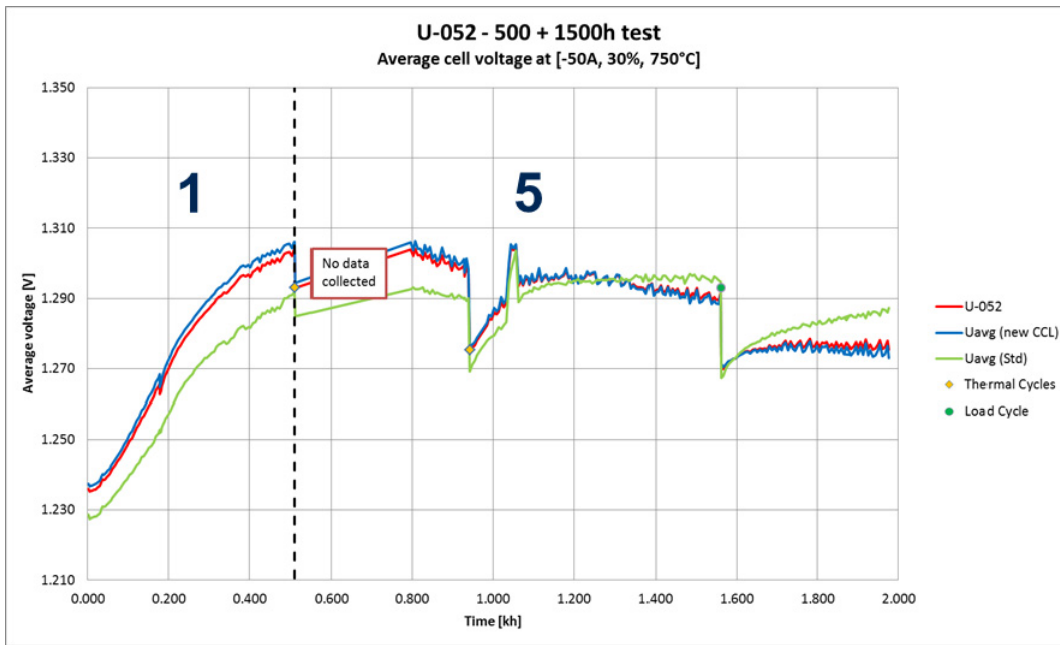


Figure 14: Average cell voltage evolution during the 500 h + 1500 h durability test. The cell voltages have been grouped to show the improved long term stability of cells with the new air side contact layer. Between sequence 1 and 5 the robustness testing (UI tests and TCs shown in Figure 15) was conducted. Due to software issues at the test station no data were collected between 500 – 800 h, however, the stack was still in operation.

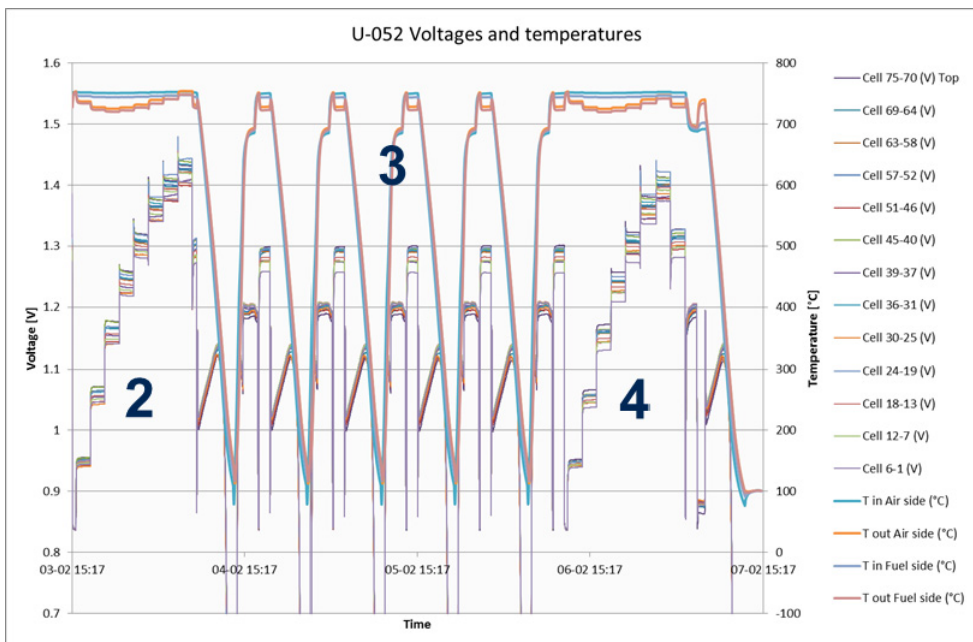


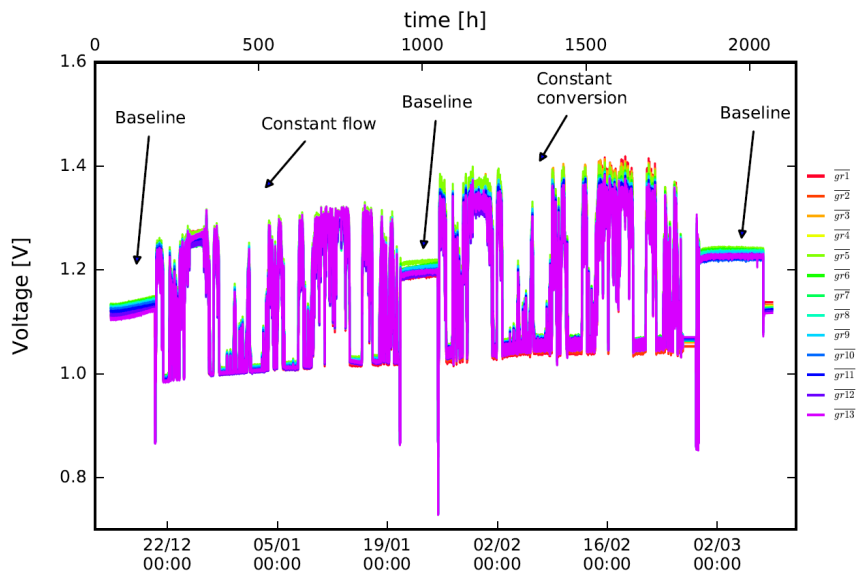
Figure 15: Cell voltages and temperature behavior during load cycles and thermal cycles.

The overview of the test results is shown in Figure 14 and Figure 15. Looking more closely at the test results, there was a similar degradation profile on all cell groups during the initial 500 h testing with a fast initial degradation, which started to level off at the end of the 500 h initial testing. Furthermore, stable operation of all cell groups at all operating points during the robustness test was also achieved. During the TCs the cell group performances were very stable with identical performance before and after the TCs, thus no degradation due to TCs. On the contrary, all cells improved in performance compared with UI test#1 (sequence 2), illustrating that a TC actually seemed to improve the stack performance. This is likely due to improved contacting between various components in the stack after a TC. During the following 1500 h test (Figure 14) there was actually a minor activation, i.e. lower cell voltage with time, with cells having the new air contact layer. Some of the activation can be explained by

a slightly higher operating temperature during the 1500 h compared with the 500 h test (not shown in this report).

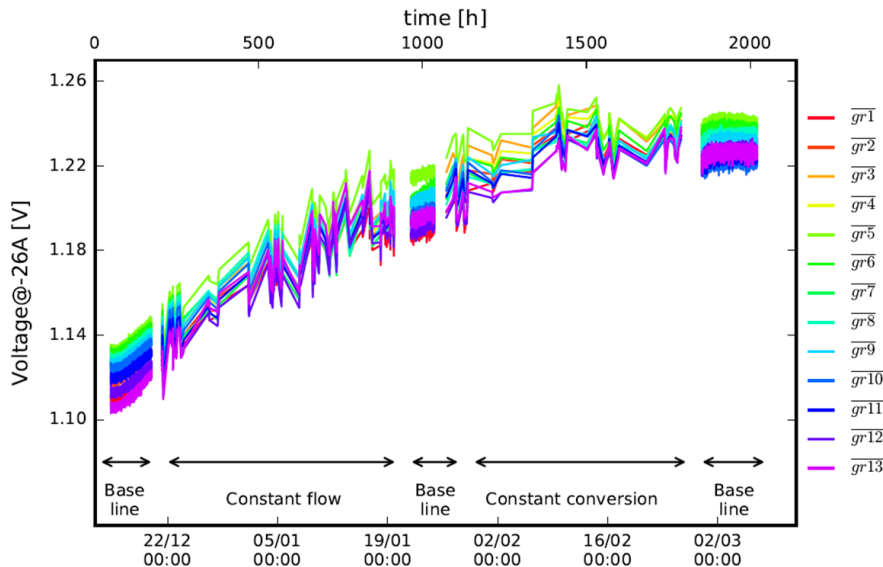
At the end of the 1500 h test the cells with the new contact layer actually had better performance (lower cell voltage) compared with at start of the long term test. Part of the performance improvement lies in the fact that one TC and one load cycle (going to OCV for a short period) seemed to activate the cells (similar to what happened during the robustness testing between the 500 h and 1500 h tests). The test confirms that the implementation of a new contact layer is promising. Post mortem analysis of the stack is being conducted to compare differences between the new and the old contact layer. The results clearly show that there is improved adhesion between the new contact layer and the air electrode.

Stack X-045 is a standard 75-cell TSP-1 stack. It was tested under the wind profile (Month December) as illustrated in Section 1.5.2 of this report, simulating 100 % absorbing wind power using the SOEC stack technology. An overview of the evolution of the average cell voltage is given in Figure 16. Figure 17 plots the average cell voltage at -0.24 A/cm^2 .



rig47_Q674_75-cells_steam_electrolysis_C:/Users/jehq/47test006/fuelcon export/SOEC_wind_26A_2.py

Figure 16: Evolution of the average cell voltage in Stack X-045 during the 2000 h test.



rig47_X-045_75-cells_steam_electrolysis_C:/Users/jehq/47test006/fuelcon export/SOEC_wind_26A_4.py

Figure 17: Average cell voltage of Stack X-045 when operated at -0.24 A/cm^2 .

the test here was to investigate the ability of TSP-1 SOEC stacks in absorbing 100 % wind power. The maximum current density exposed to the stack was therefore limited to -0.5 A/cm^2 and the average current density during the wind profile run was calculated to be -0.24 A/cm^2 . The stack was operated for electrolysis of steam with an input gas of $\text{H}_2\text{O}/\text{H}_2$ (90/10) to the fuel electrode. The test included 3 baseline runs at constant current each for 100 h, a wind profile run at constant flow conditions for one month, and another wind profile run at constant conversion for one month as well. For the baseline run, the stack was operated at -0.24 A/cm^2 with a 27 % conversion of steam into hydrogen. For the wind profile run at constant flow conditions, the conversion of steam into hydrogen varied with current density and was in the range of 11-56 %. The change of operating conditions happened every 5 minutes in accordance with the wind profile data. For the wind profile run at constant conversion, the flow to the fuel electrode varied with current density in order to keep conversion fixed at 27 %. The change of operation conditions happened every 15 minutes, due to the slow response of the steam generator. As shown in Figures 16 and 17, the stack showed minor initial degradation as expected and the voltage increase levelled out after 2000 h. The 2 wind profile runs seem having not introduced any additional degradation. The 75-cell TSP-1 stack handled the wind profile test quite well, demonstrating feasibility of using large SOEC stacks to absorb excess wind power.

As shown above, the tested TSP-1 stacks were robust towards the transient modes investigated in these tests (load changes and TCs). **The milestone M3.1** (Two stack tests for evaluating reliability of the 2014 generation SOEC stacks through different transient modes (SOEC/SOFC or SOEC/OCV etc.) including both load and possible temperature cycles for a period exceeding 1000 h completed) **is considered achieved**.

The second part of WT3.1 was devoted to investigating stack degradation under different operation conditions (temperature, voltage etc.). In this project two stacks (X-088 and X-075) were tested under CO_2 electrolysis conditions at -63 A and 25 % conversion, but at different temperatures (700 and 800 °C) to evaluate the effect of temperature on stack performance and durability. The stacks were of the TSP-1 stack type design containing 50 cells (similar stack components and cells) with a foot print of $12 \times 12 \text{ cm}^2$. An overview of the test results is shown in Figure 18.

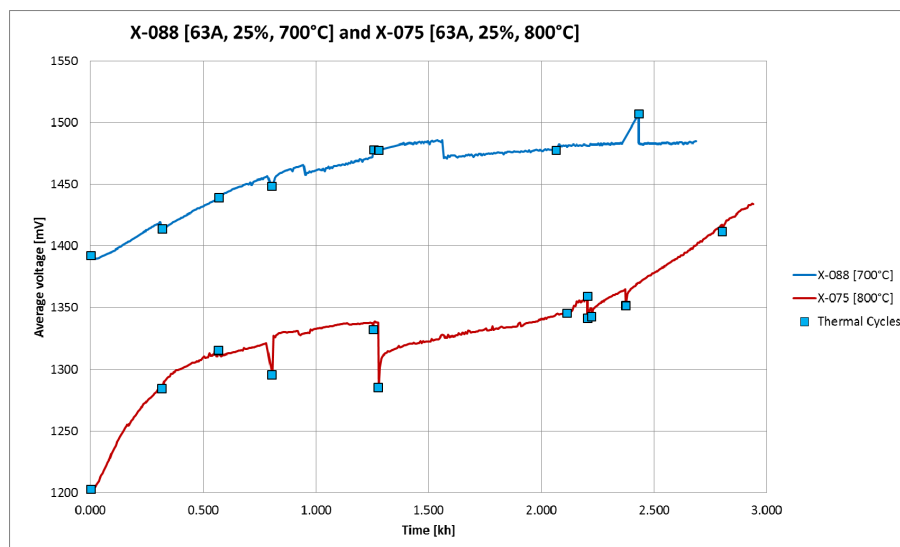


Figure 18: Average cell voltage evolution during the durability tests of X-088 (700 °C) and X-075 (800 °C).

The stacks experienced various events (test station failures) during the testing, which are illustrated by thermal cycles in Figure 18. X-075 had a high initial degradation during the first 500 h, whereas X-088 had a more smooth degradation profile that seemed to level out at around 1500 h. After 2000 h testing, X-075 operated at higher temperature started to show higher degradation rates. At close to 3000 h the stack eventually failed during a test

station event (power outage) and the stack could not be restarted. Between 2500–3000 h the degradation rate was very high (close to 10 %/1000 h). Detailed post mortem analysis of X-075 indicates that the cells had increasing leak rates with time, which is believed to be connected to the multiple test station events (thermal cycles). Thus, the stack does not seem to be robust enough for thermal cycles when it is operated at 800 °C for >2000 h.

For X-088 operated at 700 °C the situation was different. The stack was operated with a slightly different operating strategy – so-called thermoneutral test strategy. An example of the thermoneutral test strategy is shown in Figure 19 for electrolysis operation at the initial temperature of 700 °C. The average initial cell voltage was 1390 mV, i.e. < thermoneutral voltage (1.46 V for CO₂ electrolysis). As the stack degraded during the first 1500 h, the fuel outlet temperature increased due to the increase in area specific resistance (ASR). During the same time the fuel inlet temperature was adjusted from 700 °C to 720 °C to try to compensate for the increase in ASR. After 1500 h, the average cell voltage approached thermoneutral voltage, which led to a lower degradation rate and a more stable outlet temperature. At 2700 h, the inlet temperature was further increased to 727 °C, which led to a further stabilization of the average cell voltage around thermoneutral.

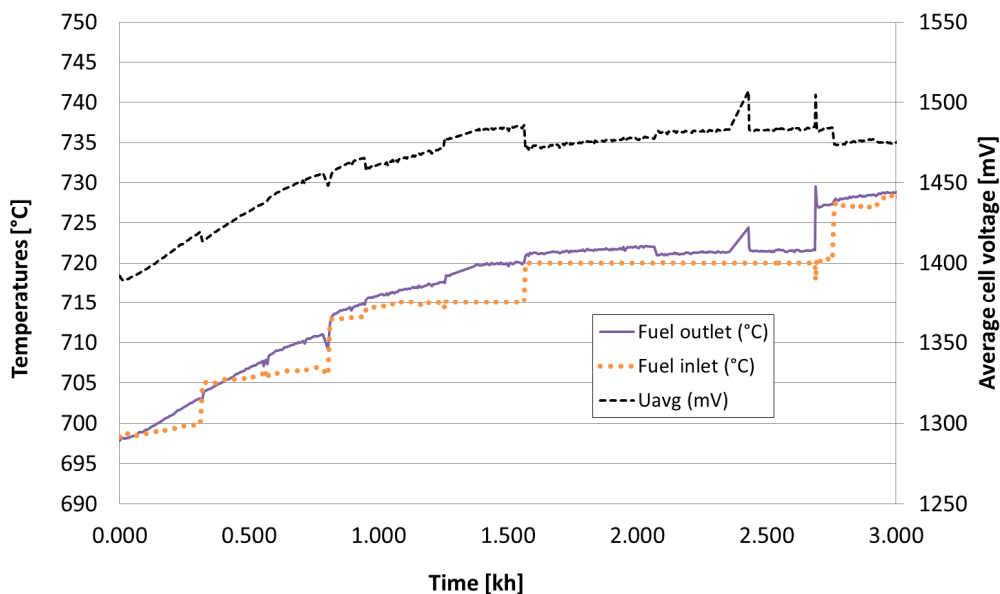


Figure 19: Stack X-088 during CO₂ electrolysis at an initial fuel inlet temperature of 700 °C.

It seems to be advantageous from a durability perspective to operate the stack with a thermoneutral test strategy. The stack was further tested to try and reach Milestone 3.6 (see below). *From these results the **milestone M3.2** (Two stack tests to investigate stack degradation under different operating temperature and/or different voltages for a period exceeding 1000 h carried out) **is considered achieved.***

The last part of WT3.1 was devoted to investigations on limits of stack operation with regard to stack operating parameters, such as temperature, current density and feed gas stream composition etc. Three stack tests were conducted within the project period. The first test was carried out on an 8-cell Delta stack (K-755) for co-electrolysis of steam and CO₂ to produce synthesis gas (syngas, CO+H₂). The stack consists of Ni/YSZ electrode supported SOEC cells with a footprint of 12X12 cm². The co-electrolysis operation was carried out by supplying a mixture of 45 % CO₂ + 45 % H₂O + 10 % H₂ to the stack operating with a fixed conversion of 39 % for steam and CO₂. The stack was operated at different conditions (see Figure 20). Initial operation at 700 °C and -0.25 A/cm² lasted for only 120 hours due to severe degradation of the bottom cell. Regaining the stack performance was realized by increasing the operation temperature to 750 °C. After reactivation, the stack showed negligible degradation at 750 °C and -0.25 A/cm² and about 1.4 %/1000 h performance degradation at 750 °C and -0.5 A/cm². The current study indicates that for the Delta stack design, -0.5

A/cm² is the upper limit with regard to current density for co-electrolysis operation at 750 °C, if a lifetime of >2 years is required.

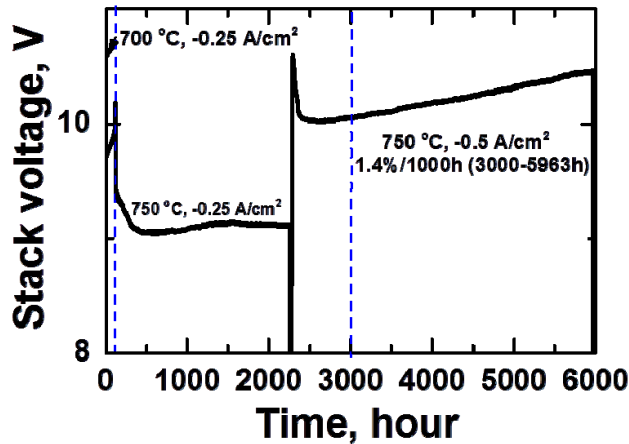
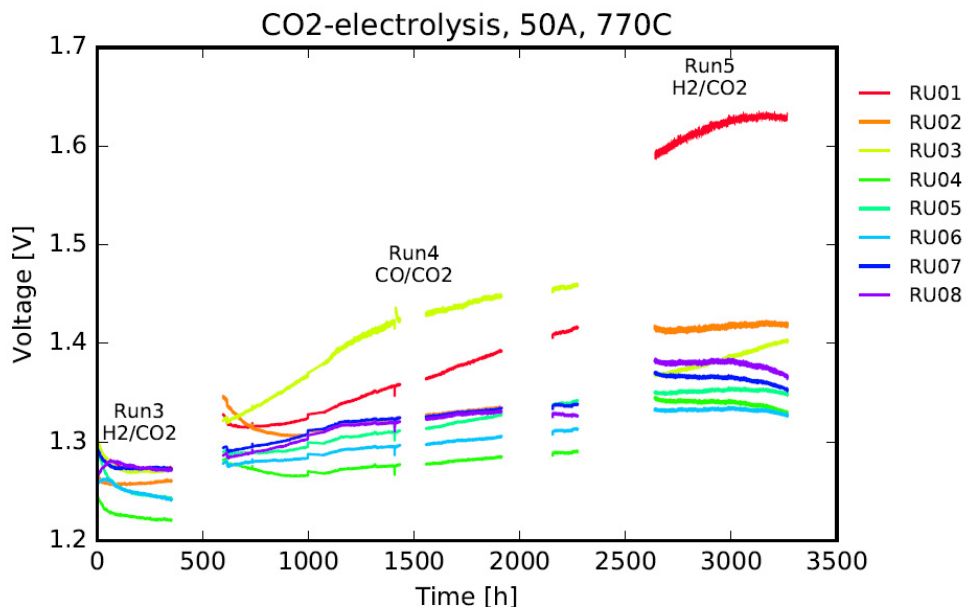


Figure 20: Evolution of the stack voltage during the durability test of K-755 for co-electrolysis of steam and CO₂.

The second test was done on an 8-cell TSP-1 stack (Q-657), which is an experimental stack optimized for performing impedance spectroscopy. The stack was tested for CO₂ electrolysis at 770 °C for more than 3000 h. An overview of the average cell voltage when the stack was operated at -50 A is shown in Figure 21. In the overall analysis the RU01, 02 and 03 is disregarded as they show erratic behavior due to contact problems. RU stands for repeating unit, which includes cell, IC, and the interfaces. An important finding is that there is no degradation in the two H₂/CO₂ runs whereas the CO/CO₂ run shows degradation. Another main finding is that the RU's degraded between the runs. Ideally the voltage should continue where it ended from the last run, however the voltages of the RU's increases both from run3-end to run4-start and again from run4-end to run5-start. The temperature is not measured in exactly the same way in run3, 4 and 5 so a lower temperature of the previous run might be an explanation for the degradation between the runs. It is speculated that the higher degradation in CO/CO₂ compared to H₂/CO₂ could be due to both local coke formation and/or a higher sulfur content in the CO/CO₂ mixture. This could be explored further in a new experiment by e.g. cleaning of the CO gas.



rig47.Q657,8-cells,CO2-electrolysis/home/ehq/47test003/compare three tests/Compare 50A 2.py

Figure 21: Overview of the average cell voltage for Stack Q-657 when operated for CO₂-

electrolysis at -50 A for run3, 4 and 5.

The third test was to explore the reliability of the TSP-1 stack at higher current densities. A 75-cell TSP-1 stack (U-053) was tested at -85 A, 35 % conversion in CO₂ electrolysis for >500 h. The stack U-053 has similar components as in U-052 (new air-side contact layer and improved gas flow distribution). An overview of the test results is shown in Figure 22. The stack showed very fast initial degradation during the first 300 h – then stabilized at approximately 1.44 V. There were also some cell voltage fluctuations, most likely related to contact issues with standard contact layer. The cells with new contact layer were less affected. This shows that the new contact layer is promising with respect to tolerating higher current densities. Comparing with U-052 tested at -50 A, 30 % conversion, Stack U-053 can tolerate higher current without being damaged, at least during the tested period. A similar total voltage increase after 500 h for the two stacks (approx. 70 mV) was observed. At the same time as the cell voltage in U-053 flattens out, the temperature difference across the stack reaches close to isothermal. It is speculated that the higher local current density in U-053 gives higher initial degradation rate due to faster “equilibration” of contact interfaces (oxide scale formation) and/or different interface composition when higher current is used.

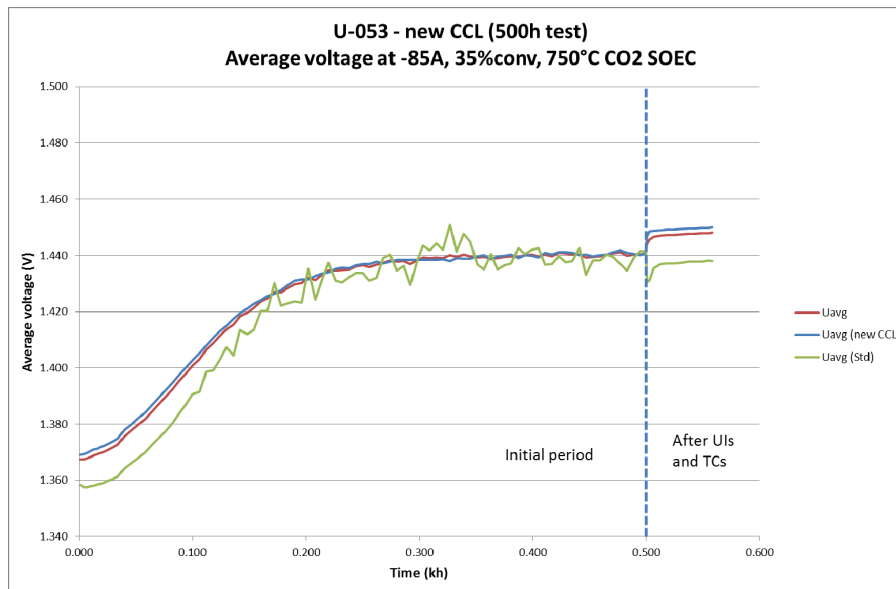


Figure 22: Average cell voltage evolution during the initial testing of U-053. The cell voltages have been grouped to compare the behavior of cells with the new and standard contact layers.

From these results **the milestone M3.3** (Two stack tests to investigate limits of stack operation with regard to possible stack operating parameters such as feed gas stream composition, conversion rate for steam/CO₂, current density etc. over a period exceeding 1000 h completed) **is considered achieved**.

Based on the above results there are strong indications that the TSP-1 stacks (as per 2014 generation) will have a lifetime of at least one year. A stack from the same generation has been successfully operated in fuel cell mode for more than 21,000 h (still in operation). Even though it is fuel cell mode operation it is still positive with regards to lifetime considerations for cell and stack components. There is nothing from a temperature perspective (material degradation, corrosion etc.) that seem to limit lifetimes exceeding 2 years, even in SOEC mode. However, this has not been proven in tests yet. These considerations on lifetime do not take into account the improvements to the stacks that have been made in this project. With the above results, **the milestone M3.4** (Life-time prediction of the 2014 generation SOEC stacks under representative SOEC operation schemes reported) **is fulfilled**.

1.5.4.2 WT3.2 – SOEC stack testing of improved cell and stack components

WT3.2 had two sub-tasks:

- To test improved SOEC cells or stack components developed in WP1 and WP2 of this project at the stack level.
- To carry out one continuous long-term test (> 1 year) to illustrate the lifetime expectancies for a continuous electrolysis process running at optimum conditions.

Within the project period, two stacks (U-052 and X-131) have been tested with the aim to show improved stack performance and stability. One of the focus points has been to work on improving the air side contact layer of the cells. Loss of contact during operation or poor interfaces between the interconnect and the contact layer is considered to be both a robustness issue (able to tolerate dynamic operation) as well as a lifetime issue (low degradation of specific components or interfaces). In the previous ForskEL project (ForskEL 12013) it was shown in the PMA work on Stack X-030 that changes in the contact quality on the air side will/can lead to longer current paths (higher resistance) and/or current constrictions. These current constrictions can lead to high local electrode overpotentials, which give rise to high degradation of the cells. The main purpose of the continued work with a new contact layer was to:

- Improve the robustness of the contact point/interface between the interconnect and the contact layer.
- Maintain or preferably increase electronic conductivity of the contact layer as compared to the one currently used.

In order to reduce the risk of carbon formation, an inherent issue when performing CO₂ and/or co-electrolysis (both steam and CO₂), we have also focused our efforts to improve the gas flow distribution inside the TSP-1 stack. The gas flow optimization was done by changing the geometry of certain stack components using computational fluid dynamics (CFD) calculation as well as COMSOL stack simulations of the changed geometry (3D simulation of the entire stack). Thus, CFD was used to improve the distribution and COMSOL used to evaluate the effect on a full stack. The improved stack design enhanced the flow distribution allowing operation with higher CO₂ conversion without Boudouard carbon formation.

The overview of test results from durability testing with various stack improvements are shown in Figure 23. X-131 was one of the first stacks with the improved gas flow distribution, however, with the standard air contact layer. A stack with the improved gas distribution modification is designated TSP-1.2. U-052 was with TSP-1.2 design but with the new contact layer. As can be seen in Figure 23, all the improvements have given very positive results on the robustness and durability of the TSP-1 stack design compared with the results from X-030 in the previous ForskEL project. U-052 was tested approximately 2000h including dedicated robustness testing with various transient modes. This was reported in Milestone M3.1.

It was originally planned that a 3rd stack with improved cells from DTU Energy will be integrated into TSP-1 stacks and tested. However, due to various cell production issues this was not realized within the project period. However, based on the above-mentioned results, together with some additional tests and validation work conducted at HTAS outside this project, HTAS has now implemented and validated the improvements in a new stack design called TSP-1.3. This updated version, which is now in production at HTAS, has the improved flow distribution and new contact layers on the oxygen side. **The milestone M3.5 (Three stack tests of SOEC stacks composed of improved cells or stack components or with optimized operation strategy for a period exceeding 500 hours completed) is considered partially achieved.**

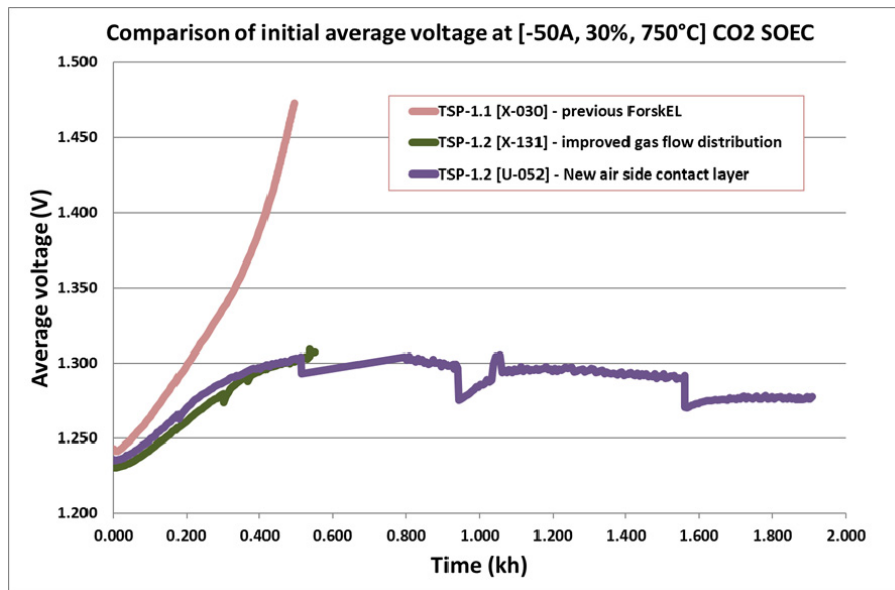


Figure 23: Average cell voltage evolution during the 500 h initial testing of stacks with various improvements. TSP-1.1 [Stack X-030] was tested in the previous ForskEL project. TSP-1.2 is the new stack version with improved gas flow distribution (also included with stacks with new contact layer).

Two 50-cell TSP-1 stacks (X-076 and X-078) were started in the previous ForskEL project and continued for some time in the current project as well. The stacks (X-076 and X-078) were tested in a dedicated test rig designed for parallel testing of 2 stacks (SOEC-CORE) at the same time (see Figure 24).

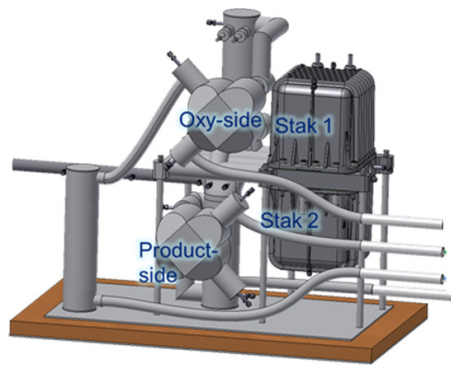


Figure 24: Schematic showing how the test rig is designed for simultaneous parallel testing of 2 stacks.

The stacks were tested with inlet gasses heated to approximately 800 °C. The stacks were tested without a furnace (adiabatic testing), which means that only the heated inlet gasses supply the heat to the stacks. The stacks were operated at -48 A and approximately 25 % conversion, with CO₂/CO on the fuel side and air on the oxygen side. The stacks were furthermore exposed to a controlled thermal cycle once per week for robustness testing. The average cell voltage evolution with time is presented in Figure 25. Stack X-078 was stopped deliberately after approximately 2700 h testing with the purpose of performing a detailed PMA of the stack. The cells had increasing leak rates with time, which unfortunately is connected to a number of test station events (thermal cycles seen as “jumps” in the cell voltage curves). X-076 continued the testing but failed after 4350 h operation, again also due to a test centre failure (power outage). Nevertheless, the stacks must be able to tolerate such events in real systems and HTAS has therefore put a lot of focus on improving the robustness of the stacks to such events.

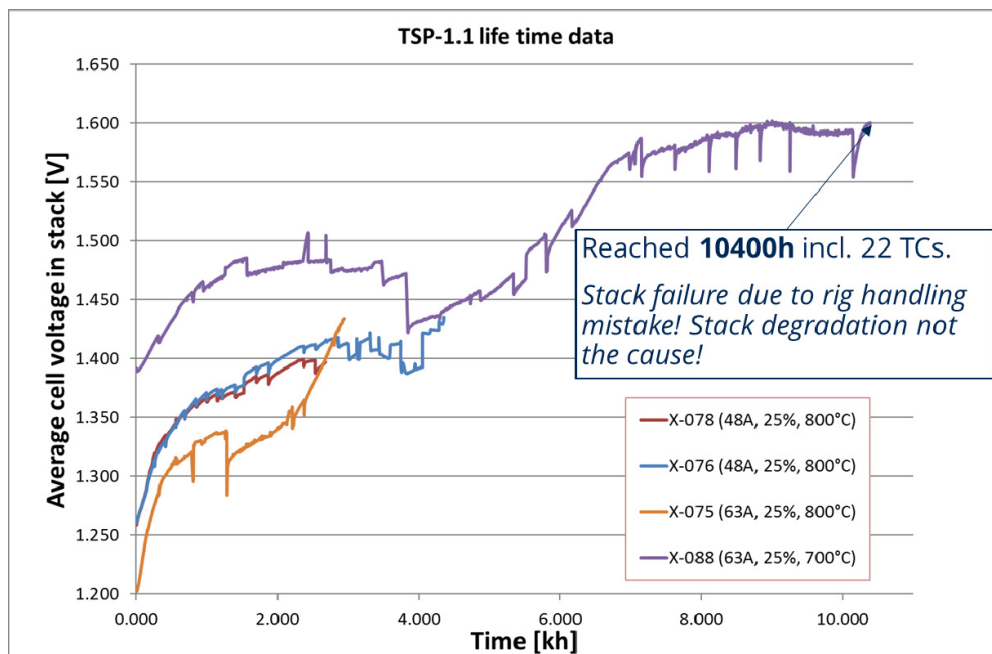


Figure 25: Average cell voltage evolution with time during long term testing of various TSP-1 stacks in CO₂ electrolysis.

The stacks discussed in Milestone 3.2 were also planned to be tested until stack failure. X-075 (-63 A, 25 % conversion, 800 °C) experienced increased leak rates with time and failed during a power outage after approximately 3000 h. Its sister stack X-088 (-63 A, 25 % conversion, 700 °C) has been operated with a thermoneutral test strategy and reached 10,400 h (see Figure 25) before it was accidentally destroyed due to a test rig handling mistake (human error causing a detrimental short circuit to the stack). Taking the whole test into account **the total degradation ended up being approximately 20 mV/1000 h or approximately 1.4 % /1000 h**. It is clear that there is a general trend that the stacks have robustness issues when they are exposed to unintentional events when they have been in operation for >3000 h. Thus, we will continue our efforts in improving stack robustness and improving the reliability of the stacks towards various unintentional system related events. Despite the failure on some of the stacks we are still pleased with the improvements done in stack operation and stack lifetime when comparing where we were at the end of the previous ForskEL project. Thus, in all the long term tests conducted it has never been the stacks failing or having too high degradation that caused a premature closure of the test. We believe that as long as the stacks are handled with care by the system, the stacks will have the potential to reach >2 years of operation without failure. However, we will continue to work with improving the robustness of the stacks in the future.

The milestone M3.6 (One SOEC stack test under optimum electrolysis conditions for a period exceeding one year with an ASR of less than $0.40 \Omega \text{ cm}^2$ and an average degradation rate of less than 1 %/1000 h at 1 A/cm^2 demonstrated.) **is considered partially fulfilled.** This milestone was formulated in accordance with the development target in the Danish electrolysis roadmap with regard to stack operation conditions. The required long-term testing at -1 A/cm^2 is not technically feasible with the current TSP-1 stack design. A more moderate and realistic test strategy for conducting the long term test was therefore chosen, which reflected the actual need for the SOEC stack development at HTAS.

1.5.5 WP4 – SOEC system

This work package involved two tasks undertaken by DTU Elektro, DTU Energy, and HTAS:

- to establish schematic designs for future SOEC plants (WT4.1);
- to develop key system components and power converters for reversible operation (WT4.2).

1.5.5.1 WT4.1 – Schematic designs of future SOEC plants

The first part of WT4.1 was devoted to identify implications of the Danish power grid and of power electronics on electrolysers. The work started with a literature review focusing on electrolyser participation in electricity markets with both transmission- and distribution-level applications, followed by a collection of typical performance data regarding electrolyser, hydrogen storage and fuel cells and an analysis of optimal size, voltage level, and participating strategy of electrolysers. Finally, scenarios regarding deployment of electrolysers in the Danish electricity grid were proposed.

To cope with the stochastic nature of renewable energy generation, energy storage (possibly in various forms, i.e., direct storage in batteries, or virtual storage through inertia of demand response) is seen as a necessary component of future power systems and electricity markets. Among various forms of energy storage systems, storage in the form of gas, including hydrogen, is seen as a viable scenario since hydrogen can be used as a clean fuel in the transport sector, and the operation process could be flexible and brings zero pollution⁶. Electrolysers are then used as the interface between the electric and gas systems, requiring appropriate sizing of the electrolyser and of the storage part. Though the previous literature studies rely on a number of assumptions and simplifications, but overall, they show interest and (economic) viability of electrolyser systems at both transmission (high voltage) and distribution (medium and low voltage) levels. In all cases, the possibility for such systems to exist, their degradation profiles, etc. are not considered and discussed, even though they are obviously key to this interface and market-related applications.

In transmission-level electricity market, players participate in market by bidding and offering. The role of the regulation power market is to ensure that generation capacity is ready to correct discrepancies between the schedules from the day-ahead and intra-day markets and the actual operation within the day. Discrepancies can arise from e.g. forecasting errors for renewable energy generation, forecasting errors on the demand side or unplanned outages of generation units. The electrolyser with hydrogen storage system could take part in the manual reserve market, which is set in place to ensure that there will be enough available bids in the regulation power market each hour. A 2009 National Renewable Energy Laboratory review on alkaline and PEM electrolyser costs⁷ concluded investment costs to be between 0.2 and 0.9 M€/MW for electrolysers with power ratings between around 0.4 and 4 MW. The report also noted that some of the costs are future projections that require future cost reductions from high-volume production. Considering the network in Denmark⁸, we can choose a 5 MW unit which works with an investment cost of 0.7 M€/MW. The operation voltage level can be 150 kV. The capacity of compressed hydrogen storage can be considered at around 4 hours of the need. The correspondent investment cost is 950 €/kg.

In distribution level, electrolyser can operate on its own and pursue the maximum profits and is controlled by an agent. The objective function is described as the following. In the distribution level network, a local market framework is established (shown in Figure 26). We consider here a common case, with participants including Distributed Energy Resources (DER), Agent in charge of operation of electrolyser and fuel cell (A), Hydrogen vehicles (HV), Load

⁶ M. Korpas, and A. Holen. Operation planning of hydrogen storage connected to wind power operating in a power market. *IEEE Trans. Energy Conversion*, 21(3), 2006.

⁷ Genovese, J., et al. "Current (2009) State-of-the-Art Hydrogen Production Cost Estimate Using Water Electrolysis: Independent Review." *National Renewable Energy Laboratory* (2009).

⁸ <http://energinet.dk/EN/ANLAEG-OG-PROJEKTER/Generelt-om-elanlaeg/Sider/default.aspx>.

(Load). The 4 participants can take part in local market as well as purchase/sell electricity energy from/to the distribution company (DisCo). Besides electricity, participants can trade hydrogen through the local market as well as with the hydrogen station. It is to be noted that, as of today, no local energy market exists, though its future existence is heavily supported by a number of projects (past and ongoing) at the Danish (e.g., iPower, TotalFlex, The Energy Collective, etc.) and European levels (e.g., Smartnet). The optimal size of an electrolyser in such a market can be decided by the aforementioned model and is highly dependent upon operational conditions, i.e., scale of the distribution network, voltage level, etc.

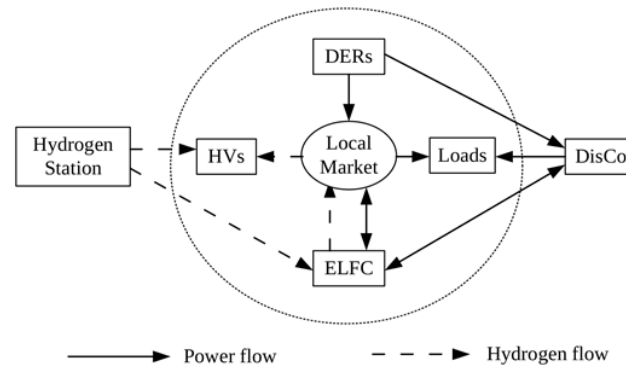


Figure 26: Local market framework, jointly for electricity and hydrogen.

Based on the above literature review and analysis, supported by our further works in ⁹ in direct relation with the current project, we envisage two possible scenarios on deployment and operation of electrolysers in power systems and electricity markets such as for the case of Denmark. On one hand, one may envisage the case of large electrolysers (MW scale) to be installed and operated at the transmission (high voltage) level for large-scale production of hydrogen and synthetic gas, also directly participating in day-ahead and regulation markets. On the other hand, small electrolysers (kW scale) could be deployed at lower network levels in combination with other distributed energy resources in the frame of local energy markets, possibly in a peer-to-peer and consumer-centric fashion. This is in line with many recent proposals for such type of markets in various Danish (e.g., The Energy Collective, EnergyBlock) and European (EMPOWER, P2P-SmarTest) projects.

The milestone M4.1 is fulfilled:

M4.1 Implications of the Danish power grid and power electronics on SOEC stacks identified and technical requirements for stack operation (in terms of voltage/current density/temperature, response time, cycling rate for transient operation etc.) reported.

The second part of WT4.1 aimed to provide schematic designs for future SOEC plants. Two application scenarios were chosen for the current study. The first is about SOEC steam electrolysis for hydrogen production. A simplified schematic of the plant model is shown in Figure 27. The schematic shows how, 1) water is taken from an external source and then mixed with recycled water that has already been through the plant; 2) the water enters a heat exchanger network where it is turned into steam and further heated towards the operation temperature of the stack using the heat of the electrolysis product streams; 3) the steam is mixed with a portion of the hydrogen-rich product stream that is recycled from the stack to prevent oxidation of nickel at the hydrogen electrode; 4) the steam-hydrogen mixture enters the stack where the steam electrolysis takes place; 5) the oxygen product stream can either be released into the atmosphere or collected after being led through the network of heat exchangers; 6) hydrogen is separated from the mixed hydrogen and steam product stream,

⁹ J. Tougaard. Participation of an electrolyzer in the power markets: with focus on the Danish day-ahead and regulating power markets. Master Thesis, DTU, 2016.

by steam condensation after passing through the heat exchangers; 7) hydrogen exits the system where it can be pressurized and stored or delivered for further chemical processing.

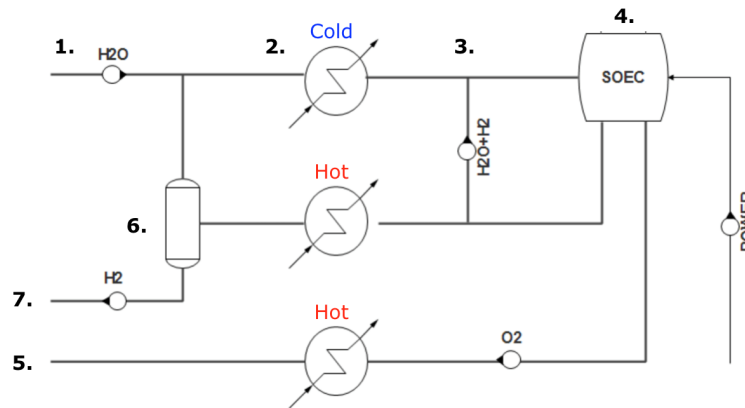


Figure 27: Simplified schematic of an SOEC steam electrolysis plant.

The second scenario is a reversible SOC plant for full energy system balancing based on the case of Danish island Ærø. In the previous project ForskEL 12013, a SOC stack was run reversibly according to a real residual curve (electricity production – electricity consumption) for Ærø island. In the current model the island is 100 % self-sufficient on energy, where electricity is provided by wind power or fuel cell operation depending on wind speed and electricity consumption, while fuel is provided through co-electrolysis followed by methanol synthesis. District heating is provided by excess heat produced mainly during fuel cell operation. Figure 28 shows how the reversible SOC system is operated in electrolysis (charge) and fuel cell (discharge) mode, respectively.

In this model the reversible SOC system is operated in electrolysis mode to produce syngas for methanol/DME production. A schematic diagram of the reversible SOC system operating in electrolysis mode is shown in Figure 29. Water and carbon dioxide are fed into the system. The input streams are heated up using heat from the exhaust streams, as well as heat from the exothermal methanol synthesis reaction. After running through the stack the syngas is led to a methanol reactor where the fuel production takes place, while the oxygen stream can either be collected or released into the atmosphere. Recycling the oxygen between electrolysis and fuel cell operation increases the energy efficiency of the reversible SOC system, but ultimately which pathway will be chosen will come down to the cost of storing the oxygen.

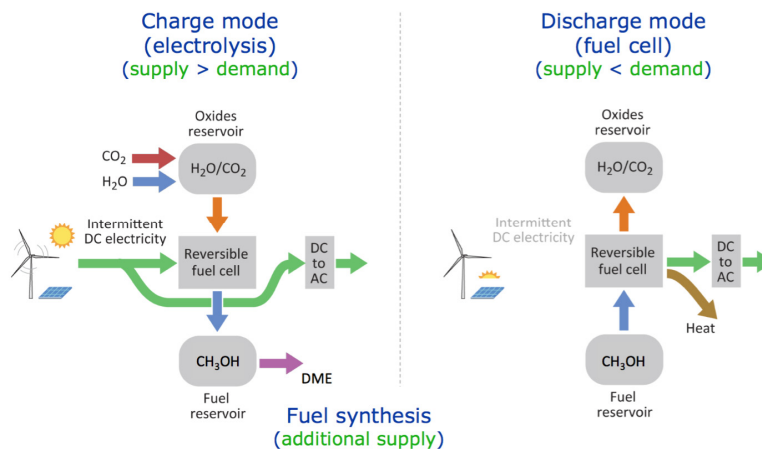


Figure 28: Illustration of the roles of different SOC modes playing in the model for the Ærø island's energy system.

During fuel cell operation (Figure 30), the reversible SOC system is fed with methanol and oxygen. However, direct use of methanol has been shown to cause serious problems with carbon formation in the heat exchange network at 600-800 °C. To circumvent this problem

the methanol is passed through a methanator and then methane is fed to the SOC system instead of methanol.

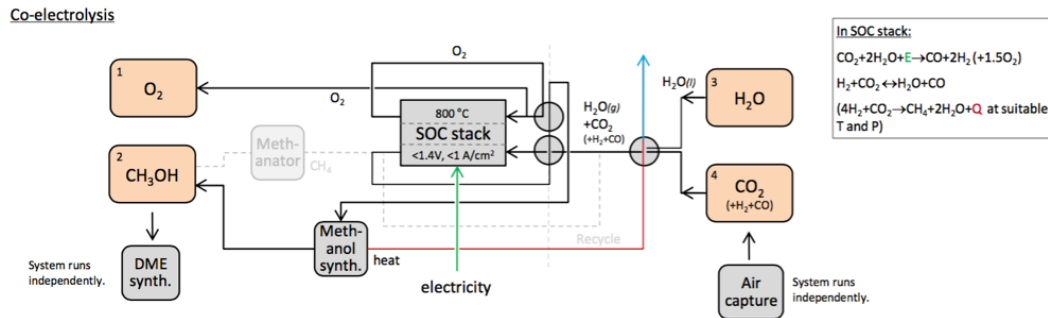


Figure 29: Schematic diagram of the reversible SOC system operating in electrolysis mode.

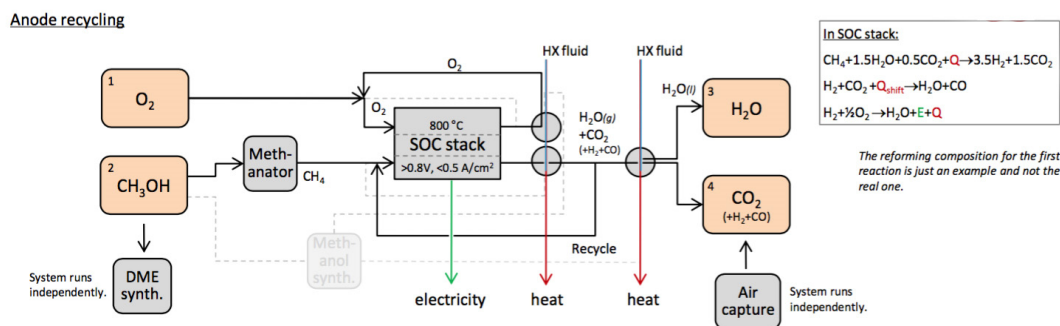


Figure 30: Schematic diagram of the reversible SOC system operating in fuel cell mode.

The milestone M4.2 is fulfilled:

M4.2 Schematic designs of future SOEC plants for at least two application scenarios (e.g. reversible SOEC/SOFC operation for grid balancing, SOEC enabled syngas production, or SOEC enabled synthetic fuel production etc.) established.

1.5.5.2 WT4.2 – Key system components

The first part of WT4.2 was devoted to SOEC-CORE systems. It was realized that it is relevant from a system perspective to properly evaluate the temperature profile and potential heat losses occurring in a system. An SOEC-CORE system will not be operated in a furnace, but inlet gasses are merely heated with heaters and heat exchangers. A proper mapping of the temperature profile of the stacks during operation is a crucial first step in a better understanding in the heat losses occurring in a system in order to develop improved heaters, heat exchangers, and thermal insulation in future systems. A specific test was set up with two TSP-1 stack tested in a SOEC-CORE. One of the stacks was equipped with 16 additional thermocouples on the surface of the stack casing. The stack was tested in a CORE together with a sister stack and tested at various operating points (*T*, conversion, current). The results from the test and comparison with the COMSOL stack model are shown in Figure 31.

There was generally a good agreement between measured and simulated casing surface temperatures. Bottom and middle casing temperatures were within 6°C – on both sides of the casing, whereas the top part results were a little more off, with COMSOL temperatures up to 16 °C hotter. Generally, the measured temperatures were similar on the two casing sides with only slightly better match with measured temperatures towards CORE components. The results showed that the COMSOL stack model should be improved to include a larger heat loss from the top of the stack. The heat loss from the casing is considered acceptable and the thermal interaction with system components (heat exchanger + heaters + tubes) is minimal.

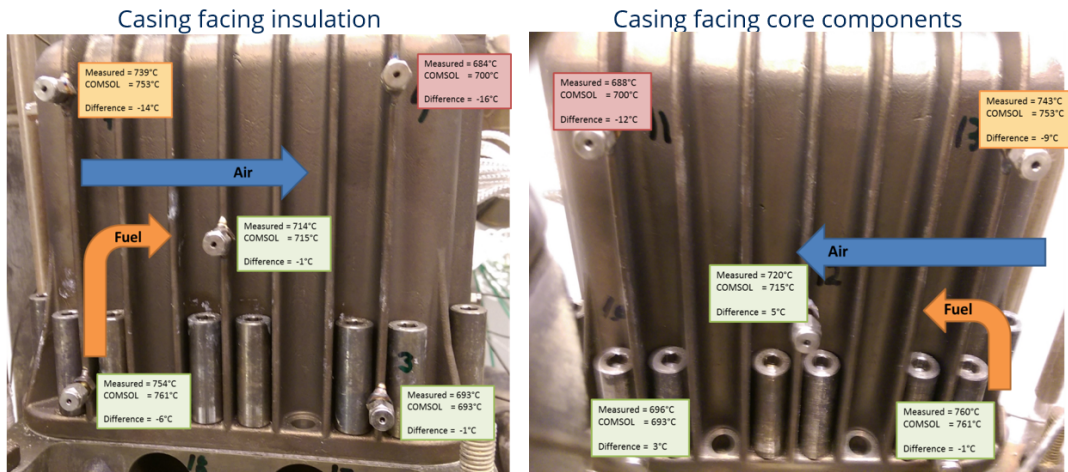


Figure 31: Results from the CORE test compared with COMSOL model results, comparing the temperature from the experimental data with values from the simulations.

These results were then used as input for developing and constructing an improved SOEC-CORE system (with respect to improved heat distribution, lower pressure drops across components etc.). Figure 32 presents a picture of the new improved CORE developed within this project. The most essential difference to the previous CORE design is the use of improved heaters and heat exchangers to tolerate higher flows. The CORE is also constructed for easy stack access for being able to exchange stacks in a simple way. To test the insulation and heat loss of the components and stacks during operation a number of thermocouples were installed on the surface of the CORE box. The measured surface temperatures were all between 30-60 °C during operation, which is acceptable and shows that the thermal insulation of the CORE box is OK. Furthermore, there were low heat losses from the heaters to the stacks (inside the CORE box) with a temperature difference of 10-20 °C. The heat losses from the stacks themselves were also measured at open circuit voltage operation. The temperature difference across the stacks was acceptable with a temperature difference (inlet to outlet) between 10-20 °C, which shows that the thermal management of the stacks inside the CORE box is good. *Thus, the outcome of WT4.2 (Milestones M4.3+M4.4) is that HTAS now has a new improved CORE design which will be used in future systems.*



Figure 32: The new CORE in place for testing at HTAS test facilities.

The milestones M4.3 and M4.4 are fulfilled:

M4.3 Temperature profiles of a SOEC-CORE system in operation acquired and compared with model simulations.

M4.4 Performance of an enhanced SOEC-CORE system tested.

The second part of WT4.2 is devoted to development of power converters for SOEC/SOFC reversible operation. Power conditioning topologies can be used to realize SOEC/SOFC systems' grid-tie operation. A simplified grid-tie power conversion architecture is illustrated in Figure 33, where the system consists of an AC-DC rectifier and a bidirectional DC-DC converter; both are based on the parallel connection to SOEC/SOFC stacks. Moreover, reversible power flows between the grid and the SOEC/SOFC stacks require full-power rating power electronic converters, i.e. the power electronic converters must be designed to have the same maximum power as the SOEC/SOFC stacks.

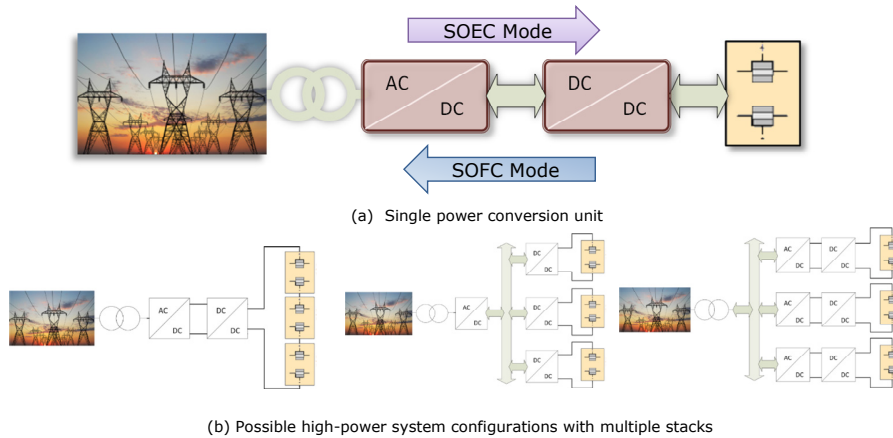


Figure 33: Traditional power conversion unit architecture for SOEC/SOFC systems.

However, I-V characteristics of SOEC/SOFC stacks differ from traditional power sources/loads. As an example, the typical power characteristics of a single cell and four stacks in series with 75 cells per stack are given in Figure 34. Based on the SOEC/SOFC stacks characteristics from Figure 34, the system specifications for the DC-DC converter using the traditional power condition unit (PCU) architecture are specified in Table 4. With the traditional architecture from Figure 33a, a 27 kW power rated DC-DC converter would be required to cover the whole power range in both operation modes. This clearly leads to an oversized DC-DC power converter when operating in SOFC mode, which only requires a 6.3 kW rated system.

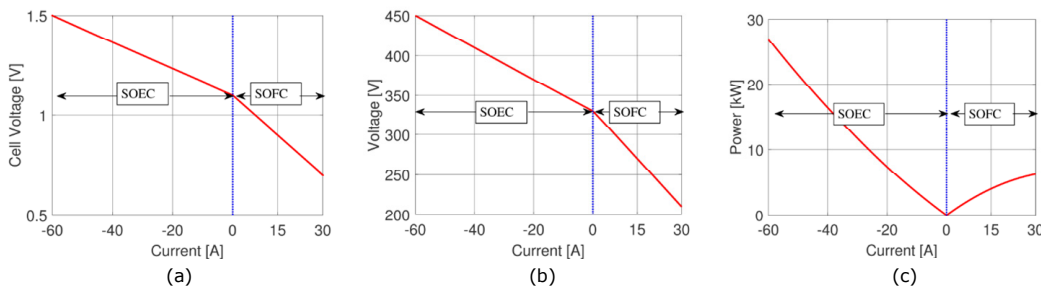


Figure 34: Characteristics of SOEC/SOFC cells and stacks. (a) V-I curve of the single cell, (b) V-I curve of the stacks and (c) P-I curve of the stacks.

TABLE 4: Traditional PCU architecture: SOEC/SOFC and DC-DC converter specifications.

Specification	SOEC	SOFC	dc-dc converter
Voltage [V]	330 - 450	210 - 330	210 - 450
Current [A]	0 - 60	0 - 30	0 - 60
Power rating [W]	27000	6300	27000
Power flow	from the grid	to the grid	bidirectional

In this project we developed a novel PCU architecture aiming to achieve a much more symmetrical power operating range of DC-DC converters. The architecture is based on a dynamic PCU which connection varies according to the operation mode by the utilization of two single-

pole-double-through (SPDT) relays as subsequently explained. The proposed PCU architecture for both operation modes is shown in Figure 35.

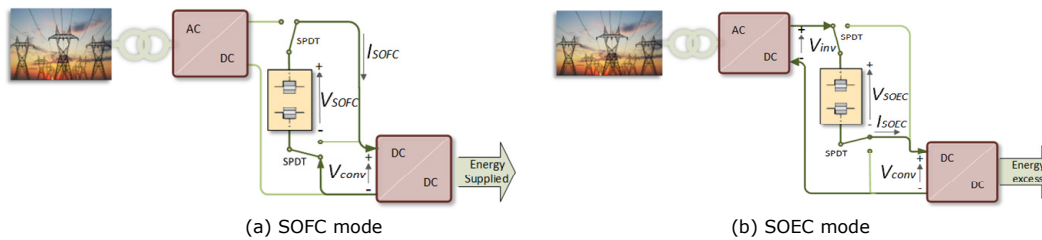


Figure 35: Novel doubly-fed power conditioning architecture for SOEC/SOFC.

Under SOFC mode, the stacks are connected in parallel to the DC-DC converter, which is the same scenario as with the traditional PCU architecture. Therefore, the power rating of the DC-DC converter is equal to the power generated by SOFCs. Under SOEC mode, stacks are connected in series with the DC-DC converter, and these two are then connected in parallel with the AC-DC converter. Energy required for the electrolysis of water and hydrogen generation is supplied from the grid through the AC-DC converter. For this operating mode, the power rating of the DC-DC converter is the power difference between the output power of the DC-AC converter and the power consumed by the SOECs. According to the stacks' characteristics from Figure 34, system specifications for the DC-DC converter and the SOEC/SOFC stacks using the proposed PCU architecture can be redefined. Calculations show that using a DC-DC converter rated at 6.6 kW, a 27 kW-SOEC/6.3 kW-SOFC system can be realized using the proposed PCU architecture. In other words, in both SOFC and SOEC modes the DC-DC converter maximum power is the same and only 6.3 kW instead of 27 kW in the traditional system configuration, resulting in not only a much more symmetrical DC-DC converter I - P characteristic, but also clearly a four times lower rated power system and thus reduced cost, losses, size and cooling effort.

In order to verify the proposed PCU solution and therefore implement tests with SOEC/SOFC stacks, DC-DC converters were designed and tested at DTU Elektro. Two types of DC-DC converters were designed, constructed, and tested in this project: a three-phase interleaved Boost converter (IBC) and a dual-active-bridge (DAB) converter. All the designed converters have been completely tested in DTU Elektro's laboratory, in terms of steady-state operation, dynamic operation and efficiency. Experimental tests have been carried out independently for each operating mode. Tests under SOFC mode have been executed simply using a laboratory power supply at the DC-DC converter input and an output resistive load emulating the power demand from the DC-link side. Tests under SOEC mode have been carried out using a DC source to supply the AC-DC converter output voltage and an electronic load in fixed voltage mode with a dynamic resistance emulating the SOEC stacks power consumption. The designed 4 kW IBC converter has a maximum efficiency of 97.3 % and 97 % under SOFC operation at 40 % load and under SOEC operation at 50 % load, respectively. More importantly, adopting the proposed novel system configuration, the 4 kW converter is able to operate a 30 kW SOEC/SOFC system, and based on the loss analysis, the whole PCU's efficiency therefore can be above 99 %. The designed 5 kW DAB converter can achieve maximum efficiency of 96.5 %, and its control has been tested not only with power supplies and loads, but also with a real 14-cell SOFC stack from HTAS.

The test of the designed DAB converter connecting to a SOFC/SOEC stack was carried out at DTU Energy. The test setup, the SOFC/SOEC cell voltage monitor equipped in the SOFC/SOEC system, and the IV -curve of the undertested SOFC/SOEC stack are shown in Figure 36.

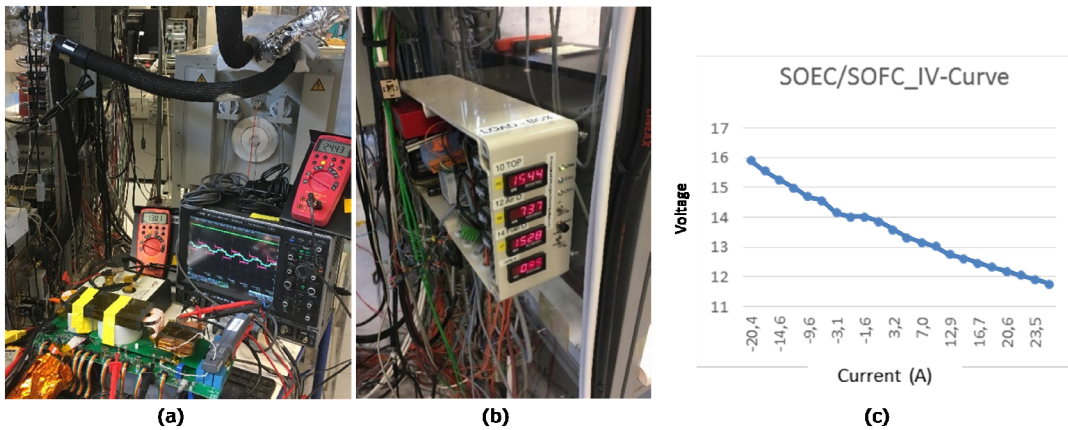


Figure 36: Test setup and SOEC/SOFC IV curve tested by the designed DAB converter.

Finally, the novel doubly-fed power conditioning architecture for SOEC/SOFC proposed in this project was tested and verified in the setup with the real SOC stack connected. The block diagram of the testing setup is simplified and illustrated in Figure 37a, and the experimental waveforms are given in Figure 37b and 37c where the red is the SOEC stack voltage V_{stack} , the yellow is the converter input voltage V_{DC} and the green is the stack current i_{stack} , respectively (time: 64 ms/div). Based on the test results, we can verify the effectiveness of the proposed power conditioning architecture, converter design and its closed-loop control, and we can conclude that:

- Power of the DC-DC converter is only half of the SOEC stacks in this case, and when we control V_{DC} to a lower voltage, the power processed by the DC-DC converter can be reduced even further;
- The DC-DC converter is well regulated, and the stack current can be controlled by the DC-DC converter (current step-down from 3 A to 1.5 A, and current stepdown causes V_{stack} decrease due to the SOEC's V - I characteristics, and accordingly V_{DC} increases).

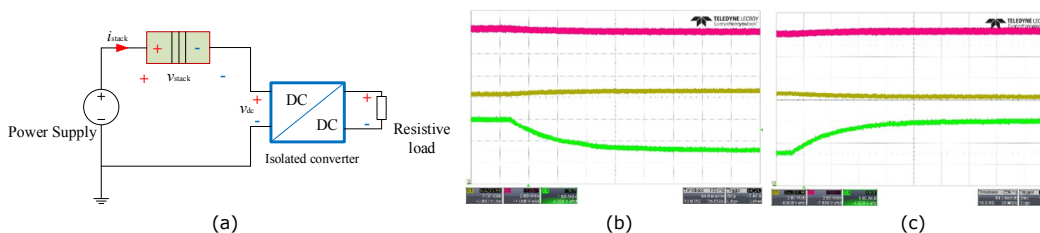


Figure 37: Test of proposed novel power conditioning architecture. (a) setup, (b) current step-down, and (c) current step-up.

Due to the complexity of the SOEC-CORE system, the integration of the designed converter into the 10 kW SOEC-CORE system was not realized in this project. However, the 5 kW DAB converter developed in this project has demonstrated a maximum efficiency of 96.5 % and its control has been tested with a real 14-cell SOC stack, showing promising results and potential in integration into SOEC-CORE systems in future projects.

M4.5 is therefore considered partially fulfilled:

M4.5 Performance of a reversible power supply unit integrated with a 10 kW SOEC-CORE system tested.

1.5.6 WP5 – Energy system modelling

The utilization of electrolyzers for grid balancing is crucial for the integration of gas infrastructure with electricity markets and the transportation sector. This was analysed by AAU in WP5 from an energy system point of view.

The first part of WP5 was devoted to the analysis on the role of electrolyzers on electricity markets in an international energy market context towards 2020 (short-term) and 2020-2035 (long-term). For the short-term role of electrolyzer in electricity system balancing, it can be concluded that electrolyzers are not expected to participate in the market-based balancing reserves in 2020, as alkaline electrolyzers are not technically suitable for the required fast regulations. With the implementation of SOECs, their participation in the balancing reserves could occur. However, this will most likely not be required as there are number of other flexible technologies that could be used instead due to better performance and lower costs. For example, heat pumps are proved to have better performance to reduce excess electricity and reduce fuel consumption, as well as having lower costs in comparison with electrolyzers. This supports the conclusion that the role of electrolysis should be primarily for electrofuel production, as it can provide the missing link between intermittent renewable energy, resource scarcity and dependence on high-density fuels. A set of different analyses in business-as-usual Danish energy system 2020 (BAU 2020) were done in order to identify the potential of electrolysis for providing grid stability and their feasibility in the system. All analyses were carried out by testing implementation of different electrolyzer capacities in the system followed by varying the amount of integrated intermittent renewable electricity. The results indicate that in terms of per MW installed electrolyzers, it is possible to reduce forced export by 17 GWh when going from no electrolysis installed to 411 MW electrolyzers. The installed capacity of 411 MW electrolysis was tested to compare with the needed capacity to meet the 10 % renewable energy goal for transport if the fuel demand is met with electrofuels. Integration of electrolysis also helps the integration of renewable energy in the system by 3 % between none and 411 MW of capacity installed. Electrolyzers have a good ability to reduce the excess electricity production from intermittent renewable sources, but the fuel saving potential is limited in comparison to other integration technologies.

With regards to system costs, systems with electrolyzers are more expensive due to investments in electrolysis capacity and fuel production components, which entails that they provide more flexibility for the system at higher costs. The analysis shows that in comparison to other transport fuel alternatives which can meet the heavy-duty transport demand, electrofuels can offer a significant reduction in biomass demand and lower energy demand in total per fuel produced. For example, the 2G bioethanol is currently using ~65 % more biomass per fuel produced in comparison to biomass based electrofuel. This also confirms that the investment in electrolysis should be driven by the need for meeting the transport fuel demand, as their biggest contribution is for fuel production rather than for grid stability purposes. The improvement in grid stability should be seen as an additional benefit from electrolyzer integration.

The analysis for 2035 shows similar trends as for the 2020 system in terms of renewable energy integration. In order to verify that the investments are relevant, also from a carbon reduction perspective, additional analysis on associated CO₂ emission shows that investment in electrolysis results in 33 % emission reduction if 43 % of the transport liquid fuel demand (that is not suitable for electrification) is met by electrofuels. As the median product for electrofuel production is always syngas, investigation on the consequences of electrolyzers' integration on gas market was carried out. It is shown that if electrolyzers are used for transport fuel production only, there is no influence on gas trading and gas balancing in the system as the gas is redirected and utilized for further fuel synthesis. However, if the produced gas is not directly used for transport but rather sent to the grid, the analysis shows that as wind integration and electrolyzers' capacity in the system increase, the operation of power plants and CHP is reduced, resulting in a lower gas demand in the system. This implies that the increased gas production in the system as a result of increased electrolyzer capacity is not needed and the system starts exporting gas already when there are very low levels of elec-

trolysis capacity. From an economic point of view, a system that uses gas directly for fuel production is cheaper than the system that uses syngas for gas balancing purposes.

In order to test the role of electrolysis in the Nordic and European energy market context, an analysis with different electricity market prices as expected to occur in 2035 was conducted to reflect the market trades. The results indicate that the cost differences for different electricity and fuel price levels are not significant, but associated CO₂ emission savings are high. Furthermore, the utilization of alkaline electrolysis in comparison to SOECs causes a negligible cost increase, however due to the lower process efficiency, using alkaline electrolysis with the same installed capacity as SOECs results in 10 % less fuel produced.

The milestone M5.1 (Results of the assessment of the role of electrolyzers on electricity markets towards 2020 (short-term) and 2020-2035 (long-term) in an international energy market context reported) **is fulfilled.**

Electrolysis offers not only the possibility to convert electrons from wind and solar to storable chemical energy but at the same time, it offers an option for system balancing and a source of flexibility. Therefore, it is seen that electrolysis could be the enabling technology for sustainable energy scenarios with restricted biomass resources. There are different ways to use electrolysis. Electricity storage in the form of liquid or gaseous fuels (i.e. so-called power-to-gas (P2G) or power-to-liquid (P2L)), in which electrolysis is a central part, could be one of the ways to provide a much needed alternative to transport fuels. There are other potential functions for electrolysis already present on the market. The ones that are more probable to emerge in the short-term, are hydrogen for industrial purposes, niche gas markets, ancillary services and hydrogen as end transport fuel. The current analysis focused on the P2G and P2L pathways. A review of the technologies involved and their development stage were conducted and illustrated in Figure 38.

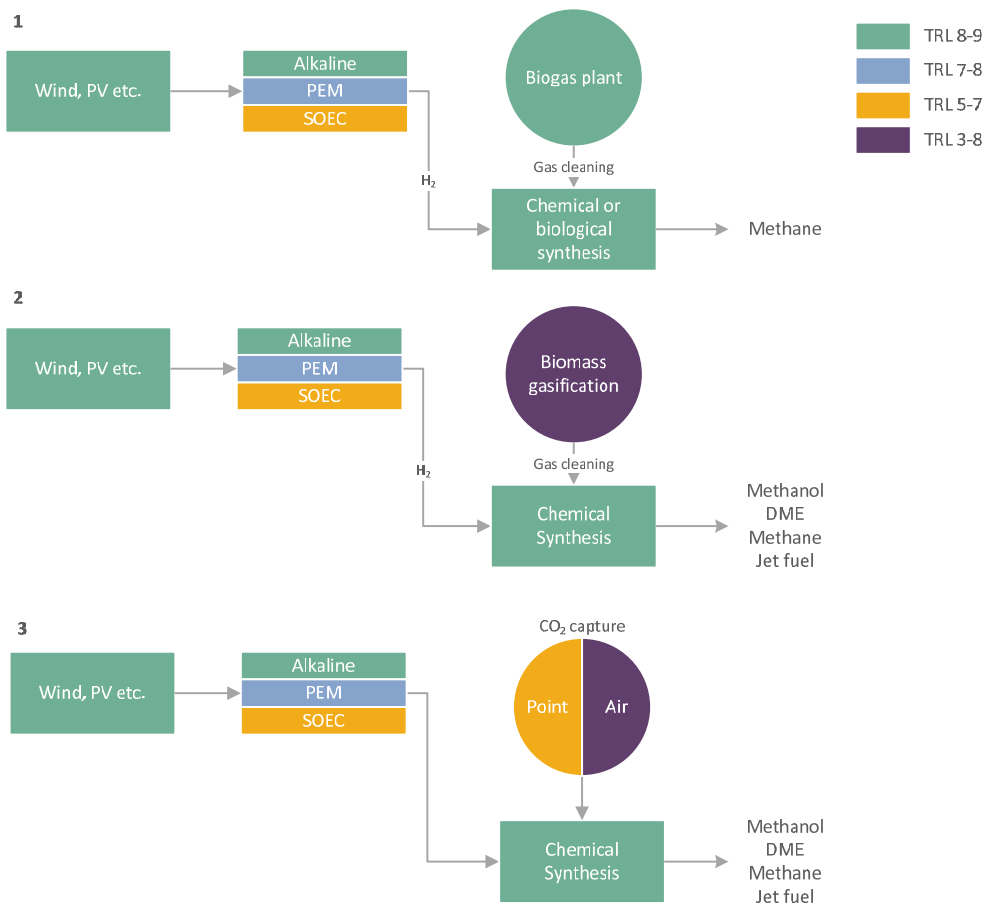


Figure 38: Power to fuel conversion processes with indicative technology readiness levels: 1) biogas upgrade with electrolysis, 2) biomass hydrogenation and 3) CO₂ hydrogenation to desired fuel products.

The second part of WP5 was devoted to creating a Danish roadmap for the development and implementation of large-scale electrolysers. The roadmap was created based on the stakeholders input, previous studies, technology status and literature review and is divided into four main stages, as illustrated in Figure 39. The roadmap further looked into different activities, measures and incentives that should be implemented in order to speed up and maximize the implementation of electrolysis. These include demonstration, regulatory measures, technology improvements and needed research.

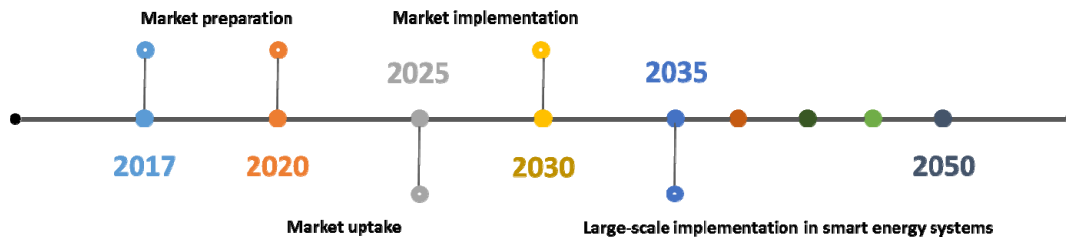


Figure 39: Roadmap for electrolysis systems from now to 2050.

Phase 1: Market preparation - from now to 2020: During the market preparation period, the goal is to develop demonstration units of electrolysers and integrate them in the production plants with installed electrolyser capacity of 1-3 MW_{el} per plant. With total installed capacity in the range of 7 and 10 MW (3 to 5 plants). Primary focus is on alkaline and PEM electrolysers as commercialized options, with transition towards SOECs when they reach desired technological level. New demonstration projects should focus on scaling up the low electrolyser capacities in the current demonstration units.

Phase 2: Market uptake – from 2020 to 2025: The market uptake phase is very important, since it will create more visibility for the technology and attract investors if the previous steps are successfully carried out. In this period, the goal is to scale up the electrolyser demonstration units to a larger MW scale. Ranging from 5 to 20 MW_{el} per plant, with total installed capacity in the 30 to 50 MW range, which would correspond to the target of 5 to 10 electrolysis based plants. It is expected that this is technically possible with commercialized electrolyser technologies because alkaline has already reached three-digit MW scale. The main barrier in practice would be the investment expenses. The business cases can be improved by changes in regulatory measures that should be introduced in the first phase of the roadmap.

Phase 3 and Phase 4: Market implementation – from 2025 to 2035 and Large scale implementation in smart energy systems – from 2035 onwards: In the period up to 2035, it is expected that both the refuelling infrastructure is in place and that fleet tests have been proven successful. This provides an opportunity to improve and expand the vehicle market. Furthermore, this can be accompanied by expanding the blend standards, availability of different fuel blends on the market, and at a few locations pure DME and/or methanol for dedicated vehicles will be accessible. This phase is also aligned with upscaling of the production facilities and electrolysis itself. It is expected that the electrolyser capacities are bigger than 50 MW and that there could be a total of 1000 MW of electrolysis integrated in the system. After 2035, the main focus is on the implementation of the technology as an active part of the smart energy system to maximize the integration of renewables and flexibility in the system. The concrete market design and conditions should be based on the experiences in the demonstration plants. A continued effort to bring the SOEC from a pilot stage to commercialization is most likely necessary.

The milestone M5.2 (Danish roadmap for large-scale implementation of electrolysers for the period 2020-2035 established) **is fulfilled.**

The last part of WP5 was devoted to establishing coherent technology data sheets for energy system analyses for the production of synthetic fuels for the transport sector with integrated SOEC, chemical synthesis, storage etc. In this task, the pathways to produce me-

thane, methanol, DME (dimethyl ether) and kerosene (jet fuel) were analyzed. The primary inputs to produce these electrofuels are hydrogen and carbon. The hydrogen is primarily obtained by using electricity and water, whilst the carbon can come from one of the following resources: combinations of animal manure and straw, biomass in the form of wood chips and other types of woody products and carbon dioxide, captured by means of carbon capture (CC) technologies. These technologies and their development status were reviewed, including electrolysis (alkaline, PEM and SOEC), biogas plants, thermal gasification, carbon capture, and fuel synthesis. By combining the above technologies, various technology pathways for the production of electrofuels, such as methane, methanol, DME, and jet fuel can be created. The potential of these technologies and the overall investment costs were then assessed.

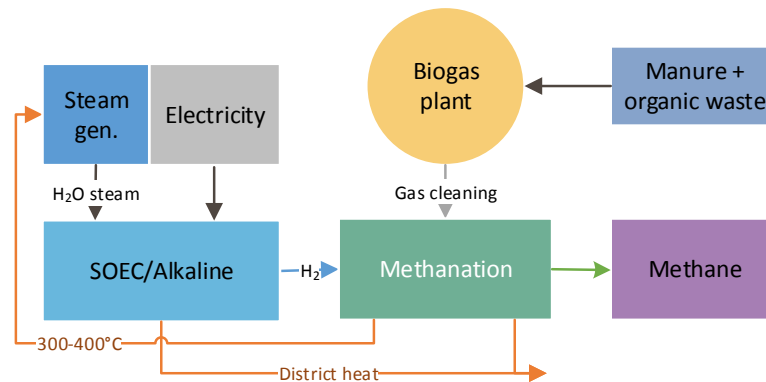


Figure 40: Biogas methanation pathway.

One example of such technology pathway is biogas methanation, as illustrated in Figure 40. The biogas produced from manure and other organic products has a high content of methane, making the biogas a product more suitable for methane production than for producing methanol/DME or jet fuel. This technology pathway has already been demonstrated in Denmark in the MegaStore project¹⁰ with encouraging results, but it has also been documented as feasible in¹¹. This pathway has been recreated in this project with the aim of highlighting the synergy to be achieved between the methanation reactor and the SOEC electrolyzers. The heat produced by the methanation reactor can be used entirely in the steam generation process for the SOEC, allowing for an increase in efficiency of the electrolyser. The increase in efficiency for the SOEC electrolyser, with the heat provided by the methanation reactor is 12 %. In the context of this technology pathway, the whole process efficiency is increased by 4 %, from 82 % to 86 %. In the case of alkaline electrolysis, the maximum process efficiency is 78 %, and no synergies can be achieved in this combination of technologies. In terms of overall costs of the pathway, these are mainly given by the cost of electrolysis and biogas plants, leaving the methanation plant at a much lower cost compared to the other two components. The cost of methane reaches €12/GJ for the year 2015 but has the potential to reduce the costs to approximately €8.5/GJ by 2050, even when no synergies are used. However, if the heat of the methanation reactor is recycled in the SOEC, then the cost can be reduced to €7.9/GJ.

The milestone M5.3 (Coherent technology data sheets for energy system analyses for the production of synthetic fuels for the transport sector established) is fulfilled.

¹⁰ MeGa-StoRE, "MeGa-stoRE," ForskEL, 2015.

¹¹ L. R. Clausen, "Energy efficient thermochemical conversion of very wet biomass to biofuels by integration of steam drying, steam electrolysis and gasification," *Energy*, vol. 125, pp. 327–336, 2017.

1.5.7 Dissemination of project results

16 oral and seven poster presentations (fully or partly supported by the current project) were given at international conferences:

1. "In-situ Diagnosis of Electrode Degradation in Solid Oxide Electrolysis Cells Using Impedance Spectroscopy", invited oral presentation given by M. Chen at the 39th International Microelectronics and Packaging IMAPS Poland Conference, Gdansk (Poland), September 21-23, 2015.
2. "Degradation and Durability of Solid Oxide Electrolysis Cells and Stacks", invited oral presentation given by M. Chen at the 3rd INTERNATIONAL WORKSHOP ON DEGRADATION ISSUES OF FUEL CELLS and ELECTROLYSERS, Santorini (Greece), September 29 – October 1, 2015.
3. "Corrosion study of ceria protective layer deposited by spray pyrolysis on steel interconnects", poster presentation given by S. Molin at the 40th International Conference and Expo on Advanced Ceramics and Composites (ICACC16), Florida (USA), January 24-29, 2016.
4. "Tracking electronic pathways in energy materials by low voltage scanning electron microscopy", poster presentation given by J. J. Bentzen at the 67th conference of SCANDEM, Trondheim (Norway), June 7-10, 2016.
5. "Relation between Shape of Ni-Particles and Ni Migration in Ni-YSZ Electrodes – a Hypothesis", oral presentation given by M. B. Mogensen at the 12th European SOFC & SOE Forum 2016, Lucerne (Switzerland), July 5-8, 2016.
6. "Long-Term Operation of a Solid Oxide Cell Stack for Co-electrolysis of Steam and CO₂", oral presentation given by M. Chen at the 12th European SOFC & SOE Forum 2016, Lucerne (Switzerland), July 5-8, 2016.
7. "Topsoe Stack Platform (TSP) – a robust stack technology for solid oxide cells", oral presentation given by J. Rass-Hansen at the 12th European SOFC & SOE Forum 2016, Lucerne (Switzerland), July 5-8, 2016.
8. "Understanding lifetime limitations in the Topsoe Stack Platform using modelling and post mortem analysis", oral presentation given by P. Blennow at the 12th European SOFC & SOE Forum 2016, Lucerne (Switzerland), July 5-8, 2016.
9. "Conversion of CO₂ to fuel and back using high temperature electrochemical cells and solar/wind power", invited oral presentation given by C. Graves at Closing the Carbon Cycle: Fuels from Air conference at Arizona State University (USA), September 28-30, 2016.
10. "Electrochemical Impedance Spectroscopy on Industrially-Relevant Solid Oxide Electrolyzer Cell Stacks: A Powerful Tool for in-Situ Investigations of Degradation Mechanisms", oral presentation given by P. Zielke at the PRiME 2016 / 230th ECS Meeting, Honolulu (USA), October 2-7, 2016.
11. "The benchmark: Electrochemistry and fuel production", invited oral presentation given by M. Chen at the 69th Annual Gaseous Electronics Conference, Bochum (Germany), October 10-14, 2016.
12. "In-situ Formed Ce_{0.8}Gd_{0.2}O_{1.9} Barrier Layer on Yttria Stabilized Zirconia Back-Bone for Infiltrated Oxygen Electrodes", poster presentation given by S. Ovtar at the PRiME 2016/230th ECS Meeting, Honolulu (USA), October 2-7, 2016.
13. "A Decade of Solid Oxide Electrolysis Improvements at DTU Energy", oral presentation given by A. Hauch at the PRiME 2016 / 230th ECS Meeting, Honolulu (USA), October 2-7, 2016.
14. "Reversible Operation of Solid Oxide Cells for Sustainable Fuel Production and Solar/Wind Load-Balancing", invited oral presentation given by C. Graves at the PRiME 2016 / 230th ECS Meeting, Honolulu (USA), October 2-7, 2016.
15. "Measurement of the fracture energy of glass-steel joints in planar solid oxide cell stacks", poster presentation given by K. Agersted at the 12th Pacific Rim Conference on Ceramic and Glass Technology, Hawaii (USA), May 21-26, 2017.
16. "Optimisation of sealing process and interfaces between glass-ceramic sealing and SOC stack components", poster presentation given by K. Agersted at the 12th Pacific Rim Conference on Ceramic and Glass Technology, Hawaii (USA), May 21-26, 2017.

17. "CO from CO₂ – on-site carbon monoxide on demand", invited oral presentation given by Peter Blennow at the 1st International Conference on Electrolysis, Copenhagen (Denmark), June 12-15, 2017.
18. "Solid Oxide Electrolysis for Grid Balancing: Recent Achievements and Future Challenges", oral presentation given by M. Chen at the 1st International Conference on Electrolysis, Copenhagen (Denmark), June 12-15, 2017.
19. "Towards long-term stable solid state electrolyzers with infiltrated catalysts", oral presentation given by S. Ovtar at the 21st International Conference on Solid State Ionics, Padua (Italy), June 18-23, 2017.
20. "Modelling of Thermally Induced Delamination in Glass/Steel Joints for Solid Oxide Cell Applications", poster presentation given by K. Agersted at the 15th Conference & Exhibition of the European Ceramic Society, Budapest (Hungary), July 9-13, 2017.
21. "eCOs – A Commercial CO₂ Electrolysis System Developed by Haldor Topsoe", oral presentation given by R. Küngas at SOFC-XV, Florida (USA), July 23-28, 2017.
22. "Systematic Lifetime Testing of Stacks in CO₂ Electrolysis", oral presentation given by R. Küngas at SOFC-XV, Florida (USA), July 23-28, 2017.
23. "Thermoneutral Operation of Solid Oxide Electrolysis Cells in Potentiostatic Mode", poster presentation given by M. Chen at SOFC-XV, Florida (USA), July 23-28, 2017.

19 papers were published in peer reviewed journals or conference proceedings:

24. D. Szymczewska, S. Molin, V. Venkatachalam, M. Chen, P. Jasinski, and P. V. Hendriksen, "Assesment of (Mn,Co)₃O₄ Powders for Possible Coating Material for SOFC/SOEC Interconnects", *IOP Conference Series: Materials Science and Engineering*, **104** [1] 012017 (2015). <http://stacks.iop.org/1757-899X/104/i=1/a=012017>
25. A. Hauch, K. Brodersen, M. Chen, and M. B. Mogensen, "Ni/YSZ Electrodes Structures Optimized for Increased Electrolysis Performance and Durability", *Solid State Ionics*, **293** 27-36 (2016). <http://www.sciencedirect.com/science/article/pii/S0167273816301643>
26. K. Agersted, M. Chen, P. Blennow, R. Küngas, and P. V. Hendriksen, "Long-Term Operation of a Solid Oxide Cell Stack for Co-electrolysis of Steam and CO₂", pp. A0804 in *Proceedings of the 12th European SOFC & SOE Forum 2016*, Lucerne, Switzerland, 2016.
27. M. B. Mogensen, A. Hauch, X. Sun, M. Chen, Y. Tao, S. D. Ebbesen, and P. V. Hendriksen, "Relation between Shape of Ni-Particles and Ni Migration in Ni-YSZ Electrodes – a Hypothesis", pp. A0902 in *Proceedings of the 12th European SOFC & SOE Forum 2016*, Lucerne, Switzerland, 2016.
28. J. Rass-Hansen, P. Blennow, T. Heiredal-Clausen, R. Küngas, T. Holt Nørby, S. Primdahl, "Topsoe Stack Platform (TSP) – a robust stack technology for solid oxide cells", Paper A1502 in *Proceedings of the 12th European SOFC & SOE Forum*, Lucerne, Switzerland, July 5-8, 2016.
29. P. Blennow, J. Rass-Hansen, T. Heiredal-Clausen, R. Küngas, T. Holt Nørby, S. Primdahl, "Understanding lifetime limitations in the Topsoe Stack Platform using modeling and post mortem analysis", Paper A1102 in *Proceedings of the 12th European SOFC & SOE Forum*, Lucerne, Switzerland, July 5-8, 2016.
30. D. Szymczewska, S. Molin, M. Chen, P. Jasiski, and P. V. Hendriksen, "CORROSION STUDY OF CERIA PROTECTIVE LAYER DEPOSITED BY SPRAY PYROLYSIS ON STEEL INTERCONNECTS", *Advances in Solid Oxide Fuel Cells and Electronic Ceramics II: Ceramic Engineering and Science Proceedings Volume 37*, 79 (2016).
31. Z. Zhang, M. A. E. Andersen, "High Frequency AC Inductor Analysis and Design for Dual Active Bridge (DAB) Converters", *Proceedings of IEEE Applied Power Electronics Conference (APEC)*, 2016.
32. K. T. Manez, A. Anthon, Z. Zhang, "High Efficiency Power Converter for a Doubly-fed SOEC/SOFC System", *Proceedings of 2016 IEEE Applied Power Electronics Conference and Exposition (APEC)*, p. 1235 – 1242, IEEE, 2016.
33. K. Kruse, Z. Zhang, M. Elbo, "GaN-based High Efficiency Bidirectional DC-DC Converter with 10 MHz Switching Frequency", *Proceedings of 2017 IEEE Applied Power Electronics Conference and Exposition (APEC)*, IEEE, 2017.
34. S. Ovtar, M. Chen, A. J. Samson, and R. Kiebach, "In-situ formed Ce_{0.8}Gd_{0.2}O_{1.9} barrier layers on yttria stabilized zirconia backbones by infiltration - A promising path to high

- performing oxygen electrodes of solid oxide cells”, *Solid State Ionics*, **304** 51-59 (2017).
<http://www.sciencedirect.com/science/article/pii/S0167273816304982>
35. A. Chrzan, S. Ovtar, P. Jasinski, M. Chen, and A. Hauch, “High performance $\text{LaNi}_{1-x}\text{Co}_x\text{O}_{3-d}$ ($x = 0.4$ to 0.7) infiltrated oxygen electrodes for reversible solid oxide cells”, *Journal of Power Sources*, **353** 67-76 (2017).
<http://www.sciencedirect.com/science/article/pii/S0378775317304706>
 36. A. Hauch, K. Brodersen, M. Chen, C. Graves, S. H. Jensen, P. S. Jorgensen, P. V. Hendriksen, M. B. Mogensen, S. Ovtar, and X. Sun, “A Decade of Solid Oxide Electrolysis Improvements at DTU Energy”, *ECS Transactions*, **75** 3-14 (2017).
<http://ecst.ecsdl.org/content/75/42/3.abstract>
 37. B. Charlas, D. W. Ni, H. L. Frandsen, K. Brodersen, and M. Chen, “Mechanical Properties of Supports and Half-Cells for Solid Oxide Electrolysis Influenced by Alumina-Zirconia Composites”, *Fuel Cells*, **17** 132-143 (2017). <http://dx.doi.org/10.1002/fuce.201600036>
 38. M. Chen, H. Alimadadi, S. Molin, L. Zhang, N. Ta, P. V. Hendriksen, R. Kiebach, and Y. Du, “Modeling of Ni Diffusion Induced Austenite Formation in Ferritic Stainless Steel Interconnects”, *Journal of The Electrochemical Society*, **164** F1005-F1010 (2017).
<http://jes.ecsdl.org/content/164/9/F1005.abstract>
 39. M. Chen, X. Sun, C. Chatzichristodoulou, S. Koch, P. V. Hendriksen, and M. B. Mogensen, “Thermoneutral Operation of Solid Oxide Electrolysis Cells in Potentiostatic Mode”, *ECS Transactions*, **78** 3077-3088 (2017).
<http://ma.ecsdl.org/content/MA2017-03/1/287.short>
 40. M. B. Mogensen, S. D. Ebbesen, S. H. Jensen, X. Sun, A. Hauch, and M. Chen, “Concentration Impedance in Testing of Solid Oxide Cells Revisited”, *ECS Transactions*, **78** 2133-2139 (2017). <http://ecst.ecsdl.org/content/78/1/2133.short>
 41. R. Küngas, P. Blennow, T. Heiredal-Clausen, T. Holt Nørby, J. Rass-Hansen, S. Primdahl and J. B. Hansen, “eCOs – A Commercial CO_2 Electrolysis System Developed by Haldor Topsoe”, *ECS Transactions*, **78** 2879-2884 (2017).
<http://ecst.ecsdl.org/content/78/1/2879.short>
 42. R. Küngas, P. Blennow, T. Heiredal-Clausen, T. Holt Nørby, J. Rass-Hansen and S. Primdahl, “Systematic Lifetime Testing of Stacks in CO_2 Electrolysis”, *ECS Transactions*, **78** 2895-2905 (2017). <http://ecst.ecsdl.org/content/78/1/2895.short>

In addition, two reports and one thesis were published:

43. I. Ridjan, K. Hansen, P. Sorknæs, J. Xu, D. Connolly, B. V Mathiesen, “The role of electrolyzers in energy system – Energy markets, grid stabilisation and transport fuels”, August, 2016, Department of Development and Planning, Aalborg University.
[http://vbn.aau.dk/en/publications/the-role-of-electrolyzers-in-energy-system\(e2a2a734-b9c1-43ee-adb0-79affac0c32\).html](http://vbn.aau.dk/en/publications/the-role-of-electrolyzers-in-energy-system(e2a2a734-b9c1-43ee-adb0-79affac0c32).html)
44. I. R. Skov, B. V. Mathiesen, “Danish roadmap for large-scale implementation of electrolyzers”, 2017, Department of Development and Planning, Aalborg University.
[http://vbn.aau.dk/en/publications/danish-roadmap-for-largescale-implementation-of-electrolyzers\(9c7c9c7e-978b-4f3f-ba9b-30b26f0cc371\).html](http://vbn.aau.dk/en/publications/danish-roadmap-for-largescale-implementation-of-electrolyzers(9c7c9c7e-978b-4f3f-ba9b-30b26f0cc371).html)
45. J. Tougaard, “Participation of an electrolyzer in the power markets: with focus on the Danish day-ahead and regulating power markets”, Master Thesis, DTU, 2016.

One popular science article about the Danish electrolysis roadmap established in this project was published in Danish news media:

46. V. B. Kærgaard, “Rapport: Elektrolyse er nøglen til fremtidens energisystem”, ENERGIWATCH, <http://energiwatch.dk/secure/Energinyt/Renewables/article9681777.ece>

1.5.8 Environmental benefits of the project

This project addressed the environmental challenges outlined in the project proposal both directly and indirectly. In WT1.3 we worked on environmentally friendly production of SOEC cells. Active layers for SOEC cells are produced by multilayer tape-casting and most tape-casting recipes contain toxic and environmentally unfriendly substances such as phthalates and strong lipophilic solvents. It is therefore necessary to pay attention to substitute these hazard substances if the fabrication of SOEC cells is to be turned into upscaled production. In this project, we replaced phthalate with a new environmentally friendly plasticizer identified in the current project and implemented in all tape-cast layers. The cells produced following the above route reached the target performance. The project hence contributed significantly to the environmentally friendly production of SOEC at DTU Energy and the newly developed production recipes can be transferred to SOEC producers such as HATS.

SOEC can produce energy carriers such as hydrogen and syngas ($\text{CO}+\text{H}_2$) which can be used for subsequent production of synthetic fuels such as methane, methanol and DME with high efficiency (above 90 %). SOEC systems have a large flexibility and modularity and have been proven to be capable of reverse and cycling operation between fuel cell mode and electrolysis mode operation. As pointed out in the WP5 work conducted in this project, the incorporation of SOEC into the future energy system will therefore ensure the possibility to incorporate larger share of fluctuating renewable energy in the energy grid aiming for the entire energy supply covered by renewable energy in 2050. It is also worthwhile to notice the potential environmental benefit that SOEC will use significantly lower quantities of toxic metals (e.g. Ni, Cr) compared with conventional batteries and no noble metals or other scarce resources are used in the SOEC. This project contributed indirectly to the above-mentioned environmental benefits by moving the SOEC technology further towards a key player in the transition to renewable energy available from around 2020.

1.6 Utilization of project results

A number of good results on the SOEC technology development have been achieved in the current project. Some of them have already been implemented in the SOEC production at HTAS, such as the improved SOEC stack and SOEC-CORE designs. The other results obtained by DTU Energy, in particular improvements in performance and durability of cells and stack components, improved understanding of degradation mechanisms, and fruitful degradation mitigation strategies will be transferred to HTAS. These results also form the basis for the necessary further research and development at DTU Energy. The power converters developed by DTU Elektro will be transferred to companies specialized in this area. With the SOEC R&D efforts spent over the last decades, commercial sales of smaller SOEC systems for on-site carbon monoxide generation have already started. The results obtained in the series of ForskEL projects including the current project played a key role in achieving the development targets necessary for commercialization of the Danish SOEC technology.

1.7 Project conclusion and perspective

The key outcome of the project can be summarized as the following:

- Lifetime prediction on 2014 generation SOEC cells and stacks with actual demonstration over 10,000 h.
- A large-scale cell fabrication technique (multi-layer tape casting) using environmentally friendly organics for production.
- SOEC cells with enhanced performance and improved long-term durability, capable of stable electrolysis operation at -1.25 A/cm^2 with actual demonstration over 6000 h.
- A new contact component which increased the interface fracture energy for one of the weakest interfaces in SOEC stacks by a factor of >2 .
- Demonstration of large SOEC stacks (TSP-1, 75 cell, rated power 7.5 kW) operated in a stable manner with a real-world wind power production profile for grid balancing purpose.
- An improved SOEC stack design (TSP-1.3) with respect to better gas flow distribution and better contacting.
- A power supply unit with a novel architecture for SOEC/SOFC reversible operation, demonstrating a maximum efficiency of 96.5 %.
- A Danish roadmap for large scale implementation of electrolyzers for the period 2020-2035.

As compared to the previous projects, significant progresses have been achieved in this project with respect to the SOEC technology development. With the 2014 generation technology, we have demonstrated stable electrolysis operation for more than one year, both at the cell level and at the stack level. We have also shown that the cells and stacks can be operated in a stable manner under grid balancing related conditions, with a realistic wind power production profile. By introducing electrocatalysts into the Ni/YSZ electrode, we were able to push the operating point for SOEC cells from -1 to -1.25 A/cm^2 with on-going cell tests running for more than 6000 h. At the stack level, we have further improved the gas flow distribution and the interface adherence and the new stack design is now implemented in HTAS stack production. The results obtained in this project are in line with the Danish national strategy and roadmap on SOEC and has further contributed to the commercialization of the SOEC technology at HTAS. Along with this series of ForskEL projects, HTAS has now matured its on-site carbon monoxide generation technology (based on electrolysis of CO_2) to a small-plant level¹². This achievement is an important stepstone in commercialization of the SOEC technology, towards the final goal of making it ready as a key player in the transition to renewable energy available from around 2020.

¹² <http://blog.topsoe.com/2016/12/site-carbon-monoxide-generation-takes-next-step>